Cózar, P., Coronado, I., García-Frank, A., Izart, A., Somerville, I.D., Vachard, D. 2022. Alternating microbial mounds and ooidal shoals as a response to tectonic, eustatic and ecological conditions (late Viséan, Morocco). Sedimentary Geology, 431, SEDGEO 106109 https://doi.org/10.1016/j.sedgeo.2022.106109

Alternating microbial mounds and ooidal shoals as a response to tectonic, eustatic and ecological conditions (late Viséan, Morocco)

Pedro Cózar[a,b,*], Ismael Coronado[c], Alejandra García-Frank[b], Alain Izart[d], Ian D. Somerville[e], Daniel Vachard[f]

[a] *Instituto de Geociencias CSIC-UCM, c/ Severo Ochoa 7, 28040, Madrid, Spain*
[b] *GEODESPAL, Universidad Complutense de Madrid, c/ José Antonio Novais, 12, 28040-Madrid, Spain*
[c] *Facultad de Ciencias Biológicas y Ambientales, Universidad de León, Campus de Vegazana s/n, 24071-León, Spain*
[d] *202 chemin de Cabanis, 34730 Prades-le-Lez, France*
[e] *UCD School of Earth Sciences, University College Dublin, Ireland*
[f] *1 rue des Tilleuls, 59152 Gruson, France*

* Corresponding author
E-mail: p.cozar@igeo.ucm-csic.es

Abstract

The succession in the Tizra Formation shows an excellent exposure of a small open marine platform where alternating microbial boundstones (buildups) and oolitic/bioclastic grainstone (shoals) and packstone facies tempestites occur repetitively for a sort interval only 0.55 Myr, an scenario unknown in the geological record. The relatively small extent of the platform allows a detailed study of facies and ecological variations, to determine the controlling factors for the growth and evolution of the platform (tectonics, glacioeustatism, terrigenous imput), as well as the particular environmental/ecological conditions for the formation of microbial buildups and oolitic shoals (turbidity, energy, nutrients, chemical variations).

Although microbial mounds are well-known during the Palaeozoic, the close relationship with ooids, as observed in the studied succession, is unusual, particularly

for the frequent ooids embedded in the microbial facies, an ecological parameter used by previous authors to identified shallower stages in the microbial growths.

Petrographic analysis of the ooids, as well as their ecological conditioning, suggest that less than 40% of samples yield ooids generated in situ, whereas there is a predominance of transported ooids. Ooids formed in situ, which include large irregular and elongated ooids, were generated in calmer water than the typical rounded and egg-shaped ooids. The occurrence of the predominant types of ooids in shallower-water grainstones with in situ generation, and in the deepest-water microbial facies, suggest their ease of transport. The higher production of ooids occurs during the shallowing phases of the cycles, whereas they were more easily transported during the deepening phases, whereas in the microbial buildups, no features of in situ ooid generation are found.

Keywords
microbial boundstones, ooids, cyclicity, syn-sedimentary faults, upper Viséan

1. Introduction

Microbial mounds and oolitic carbonate sediments are important proxies for physical, chemical and biological environmental conditions in the rock record (e.g., Whalen et al., 2012; Diaz and Eberli, 2019). Generally, they are representative of rather distinct environments, with microbial mounds accumulating in low-energy deep-water settings, whereas ooids are mostly concentrated in constant high-energy shallow-water settings (e.g., Lees and Miller, 1985, 1995; Bourque et al., 1995; Trower et al., 2017; Harris et al. 2019). However, the passage from ooidal limestones to microbial mounds, or vice versa, is well-known in Mississippian mounds (e.g., Pickard, 1992; Bourque et al., 1995; Cózar et al., 2006, 2019), but usually, they are associated with singular long-time deepening- or shallowing-upward sequences. In some cases, the transition between the ooidal deposits and the microbial mounds are interpreted as major sedimentary breaks, with each break marking an abrupt increase in water depth, and thus, a maximum flooding surface (Bourque et al., 1995). For instance, in this latter succession, thirteen transgressive-regressive cycles were defined in a succession 1500 m thick, and about 8 Myr duration. Similar microbial buildup-ooid sedimentological settings are also well known in the geological record (e.g., Adachi et al., 2009). Rarely, small microbial buildups occur within thick ooidal and bioclastic bars (Tomás et al., 2013; Lehrmann et al., 2020), being associated with punctuated and small-scale deepening-upward sequences in some precise events or intermediate-frequency cycles, but not distributed through the entire succession or in each cycle. During the Messinian, microbial buildups associated with ooidal units, in some cases interfingered, are commonly described from the Mediterranean region, but in a completely different environmental setting, because

they are interpreted as a restricted shallow marine sedimentary system with evaporites, separated from open marine conditions (e.g., Goldstein et al., 2013; Suarez-González et al., 2019).

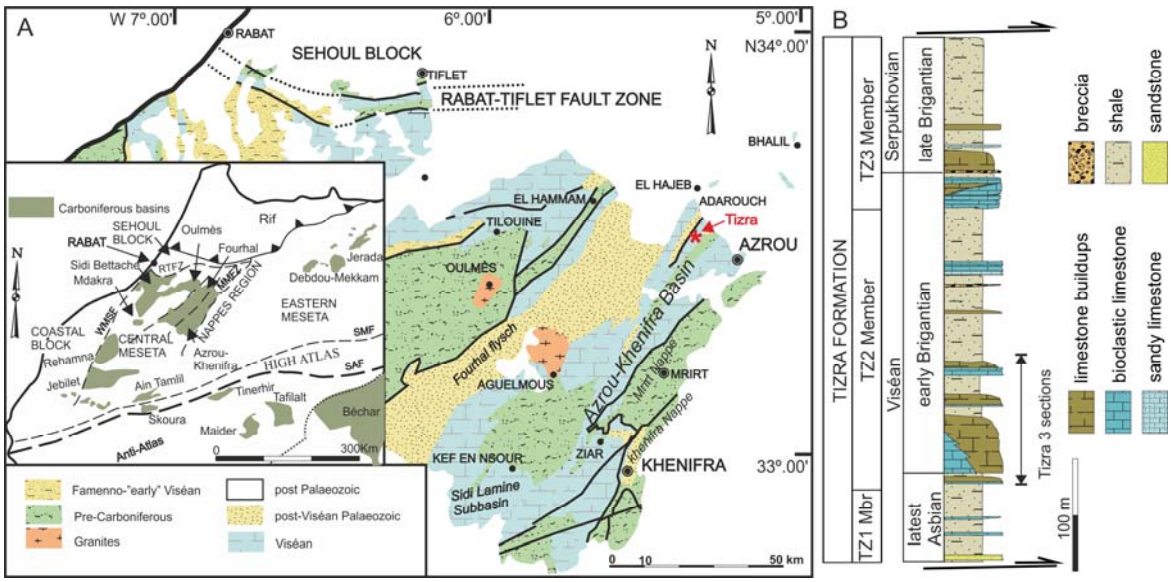

Fig. 1. A. Geological map of the central parts of the Western Meseta within the main Carboniferous outcrops in Morocco (encased box). Abbreviations: MMFZ – Middle Meseta Fault Zone, RTFZ – Rabat-Tiflet Fault Zone, SAF – South Atlas Front, SMF – South Meseta Fault, WMSF – Western Meseta Shear Fault. B. Simplified stratigraphic section of the Tizra Formation.

Apart from those occurrences or repetition of both lithologies attributed to major drops in sea-level, it is also interesting to note the different interpretation of ooids recorded within the microbial mounds. For some authors, they are regarded as allochthonous (transported by currents), occurring in the top of the mounds and frequently associated with patches of grainstones and packstone facies (e.g., Lees et al., 1985), or as cavity filling sequences (e.g., Rodríguez-Martínez et al., 2012). Whereas, for other authors, the ooids recorded at the top of the shallow-water mounds are considered autochthonous (e.g., Ahr and Stanton, 1996). This contradictory interpretation is also observed in the Messinian buildups (e.g., Villafañe et al., 2018; Suarez-González et al., 2019).

Hence, a repeated alternation of ooidal/bioclastic grainstone and microbial mounds formed under distinct environmental conditions in an open marine platform setting for short lateral distances and short time-intervals is unknown. In Morocco, both lithologies are recorded in excellent exposures of the Mississippian Tizra Formation, which allows the observation of the internal structures, morphology and architecture of the limestone units. These exposures facilitate detailed analysis of the intrinsic and extrinsic factors controlling facies variability, characterized by rapid changes, even over short lateral distances. The co-existence of both lithologies cannot be explained by any previously published model, and a single predominant factor cannot explain the succession observed in the Tizra Formation. Unfortunately, microbial mounds, such as those recorded in the Palaeozoic, are not developing currently. Instead, most microbial carbonates are associated with rather shallow-water hypersaline and stressed

environments (Friedman et al., 1974; Dupraz et al., 2009), similar to the most recent Messinian microbial buildups. Thus, there is no modern or recent analogue in open marine conditions. Furthermore, Palaeozoic microbial mounds are frequently rather monotonous successions in which there are very few sedimentological features so as to determine trends, where precursor-core-cap facies are not recorded (Lees and Miller, 1985), and microfabrics are randomly distributed. Cyclicity recorded in some Carboniferous mounds, when recognized, is described for thick successions and long-time intervals (Bourque et al., 1995), but not internally for the mounds. However, detailed statistical analysis of the skeletal and non-skeletal components within the mounds, enable us to recognize ecological gradients marking shallowing trends, or a relay index in this particular environment based on components distributions (Lees and Miller, 1995; Devuyst and Lees, 2001), even high-frequency cyclicity (Cózar et al., 2019).

The purpose of this paper is to provide mechanisms which may have controlled the genesis and alternation of microbial mounds, together with ooidal-bioclastic shoal units in Morocco, in order to test possible sedimentary breaks and major sea-level falls, as well as to determine the origin of ooids within the microbial facies. This favourable location allows both tectonics and eustatism to leave a specific imprint compared to the ecological and environmental needs for the formation and transport of ooids, as well as the precipitation of microbial buildups. Detecting which factor triggers each process can be useful for future detailed studies of other basins with similar alternation of both lithologies, as well as to reconsider some environmental interpretations of microbial mounds described in the literature based on this proxy.

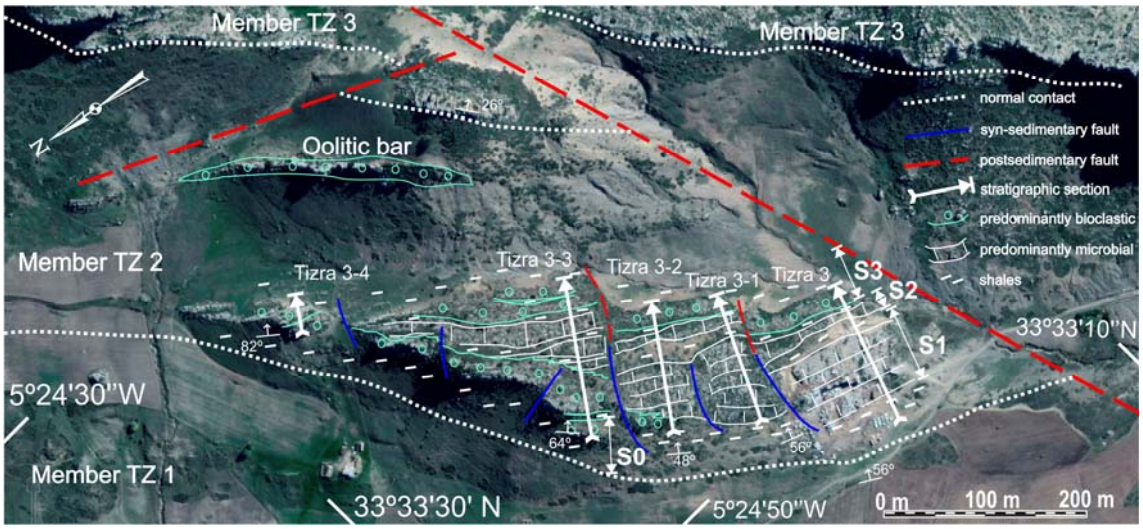

Fig. 2. Geological sketch of the members looking southeastwards, showing the main facies types and the position of the three sequences S1, S2 and S3, and location of the section (source of the image Google Earth).

2. Stratigraphical and biostratigraphical context

The Azrou-Khenifra Basin, in the Moroccan Meseta (Fig. 1), has been affected by numerous stages of magmatism, faulting, folding and tectonic/gliding nappes (e.g., Allary et al., 1976; Bouabdelli and Piqué, 1996; Ben Abbou et al., 2001). Despite Variscan deformation, Carboniferous rocks show an excellent preservation of the

geometry and distribution of the deposits, especially in the Tizra Formation in the Adarouch region (subdivided in TZ1 to TZ3 members; Figs. 1–2).

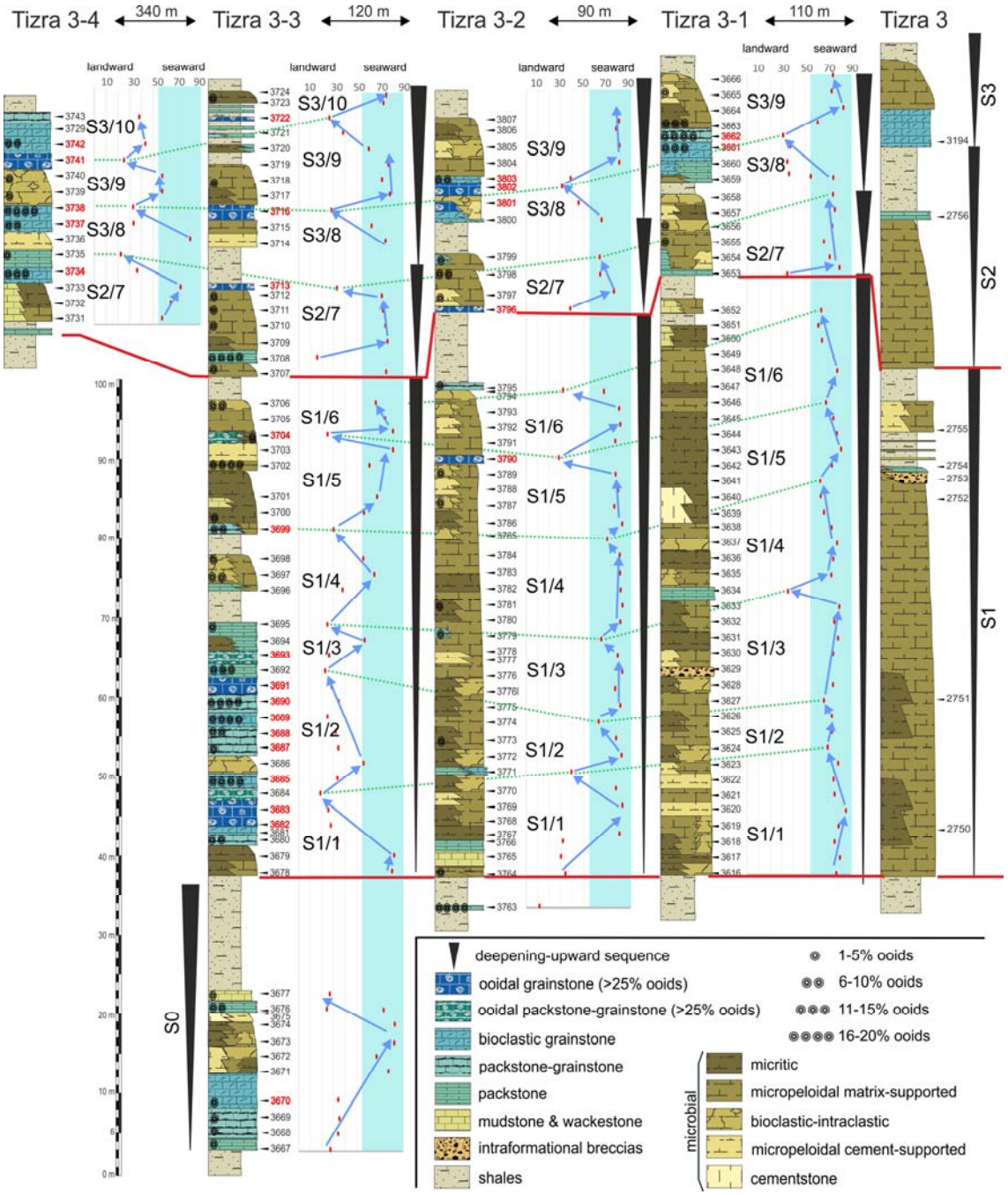

Fig. 3. Correlation of stratigraphic sections (solid lines) in the lower part of the TZ2 Member and location of sampled horizons. S0-S3 are the main overall deepening-upward sequences. Left column in each section correspond to the representation of the index I_1 on the stratigraphic sections showing small frequency cycles S1/1-S1/6, S2/7, S3/8-S3/10 and their correlation (dotted lines). Sample numbers in bold red font correspond to those yielding in situ precipitated ooids (see Table S2).

Limestone buildups occur in the TZ2 and TZ3 members, although in the upper TZ3 Member of the formation, they are rather similar to other coeval microbial mounds described from Morocco (e.g., Wendt et al., 2001; Aretz and Herbig, 2008; Somerville et al., 2012), as well as in the adjacent palaeogeographic regions of Algeria and SW Spain (e.g., Bourque et al., 1995; Rodríguez-Martínez et al., 2010). These TZ3 mounds

are characterized by a predominance of stable, deep-water conditions in the outer platform, generating relatively large domical-shape mounds with topographic relief, and dominated by micropeloidal and clotted textures (sensu Sun and Wright, 1989), and rare shallower limestones, usually attributed to intermound-offmound settings (Aretz and Herbig, 2008; Somerville et al., 2012). In contrast, the TZ2 Member presents an intercalation of microbial mounds and oolitic/bioclastic shoals , which, apparently, are both representative of very distinct environments.

In the field, three overall deepening sequences, S1 to S3, can be recognized and mapped, based on the occurrence of continuous bands of deeper-water shales at the top (Figs. 2–3). These shales are considered as a deeper-water setting due to the absence of sandstones with sedimentary structures and macrofauna, except for rare crinoids and sponge spicules. In addition, in the thick shale interval above sequence S3, slumps and debris flows are recorded. Shales below the succession are different, yielding common sandstone beds and conglomerates (with Devonian pebbles) with common sedimentary structures, and macrofossils are limited to plant remains, suggesting a deltaic setting (Karim, 2008).

In the field, it can be observed that the oolitic/bioclastic shoals developed directly on the shales to the north, and they pass southwards to the microbial mounds. The platform is intersected by small faults. During sequences S1 and S2, these faults allow a thickening of the facies from north to south (Fig. 3), even with thicker units juxtaposed to the faults, which are interpreted as syn-sedimentary in nature (Fig. 2). However, during sequence S3, the thickness of the different lithological units is uniform from north to south, and at outcrop, there is a marked displacement of these units due to post-sedimentary movement of the faults. Differences in thickness between the sequences are not all that large, ranging from 5 to 10 m, although taking into consideration the short distance between the sections, implies a significant tectonic movement in the faults.

The biostratigraphy of these rocks has been well studied by several scholars (e.g., Berkhli et al., 2001, Cózar et al., 2008, 2011; Izart et al., 2017; plus ongoing work of the authors), although its sedimentology has been less well studied (Berkhli et al., 2001; Karim, 2008). Except for the basal sandy/bioclastic TZ1 Member of the Tizra Formation, most of the limestones were described as microbially-induced ("spongiostromic limestones") and black bioclastic limestones (Berkhli et al., 2001). The thickness of these members varies from north (where Berkhli et al., 2001 analysed the succession) to south (analysed herein; Fig. 2). The TZ1 and TZ3 members crop out along-strike in a NE-SW direction more or less continuously for about 7 km, whereas limestones of the TZ2 Member occur discontinuously, since this member is dominated by shales in most parts of the region. The Tizra Formation is thrusted in its upper part (to the east) by the Mouarhaz Formation and laterally covered unconformably by Triassic rocks. The Mouarhaz Formation is coeval to the upper part of the TZ3 Member (Cózar et al., 2008, 2011), but yielding shallower water facies (nearshore conglomerates, sandstones and ooidal shoals). On the other hand, the base of the Tizra Formation (to the west), is thrust over pro-deltaic shales and sandstones of the M'Taoutoult Formation, with a similar stratigraphic range to the Tizra Formation, but reaching younger levels of the Serpukhovian.

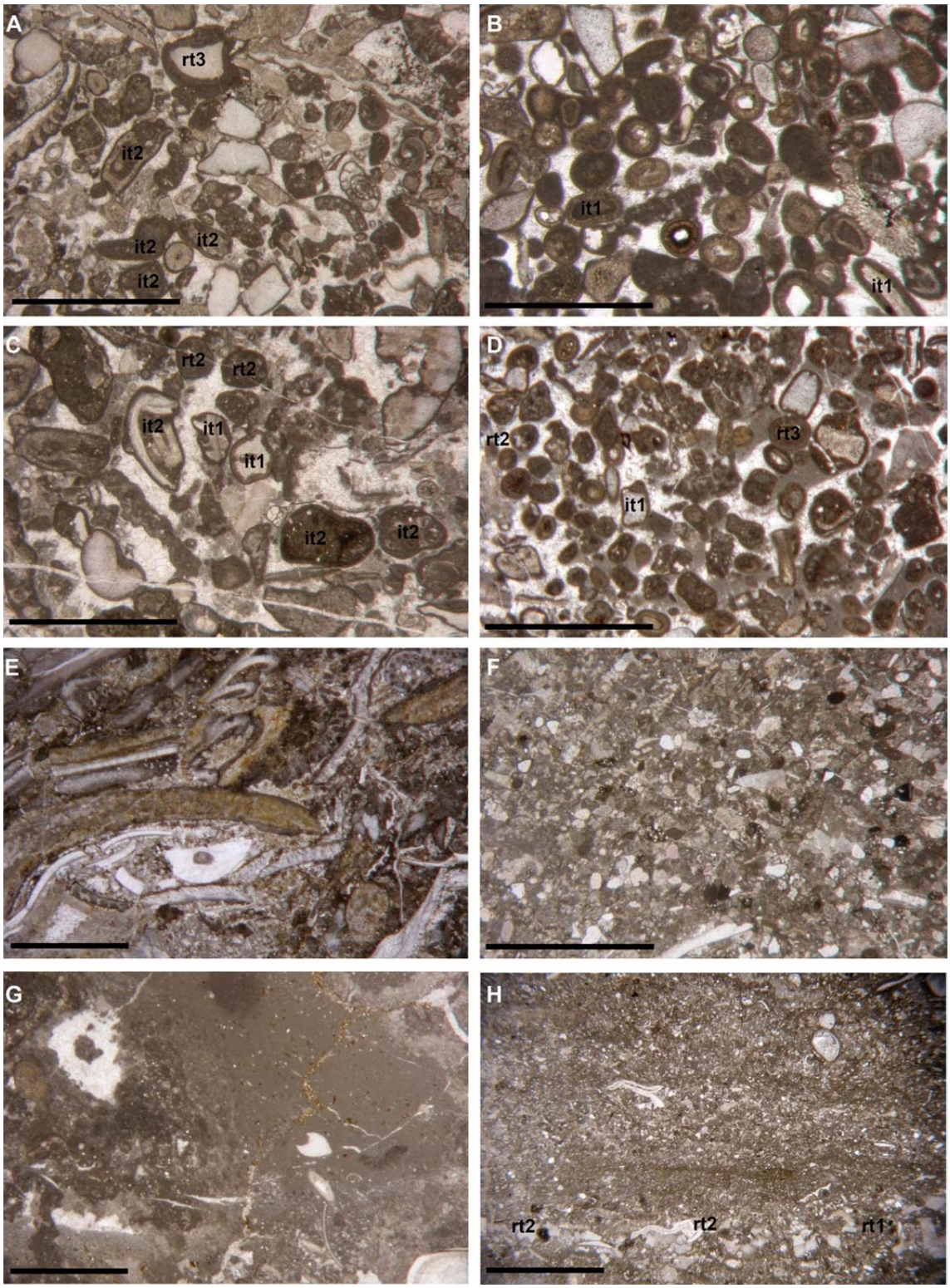

Fig. 4. Selected photomicrographs of non-microbial microfacies. Way-up to the upper part of the pictures. Scale bar = 2 mm except for figs B (= 1mm) and G (= 4 mm). A. Bioclastic grainstone with sparse micrite, showing crinoids, foraminifers, ooids (regular type 3 (rt3), irregular type 2 (it2)), brachiopods, lithoclasts. Note the thin coating on many bioclasts, especially crinoids, 3734. B. Ooidal grainstone, well sorted, most ooids of regular type 3, and some irregular type 1 (it1), with some sparse crinoids with coatings; lithoclasts and subangular quartz grains are the most common nuclei, 3722. C. Lithoclastic-ooidal packstone-grainstone, poorly sorted, mostly irregular type 2 (it2), irregular type 1 (it1) and regular type 2 (rt2), very thin, 3690. D. Ooidal packstone-grainstone, well sorted, superficial ooids predominant over tiny crinoids and intraclasts (regular type 2, 3 and irregular type 1, rt2, rt3 and it1 respectively), 3662. E. Bioclastic packstone, poorly sorted, with recrystallized brachiopods and crinoids imbricated deposited microbial micrites, 3694. F. Sandy-intraclastic-crinoid packstone at the base of the mounds, 3667. G. Micrite microbial textures (lower left) with stromatactis filled by internal sediments passing to mudstone, 3650. H. Wackestone with crinoidal packstone partings, with rare regular type 1 (rt1) and regular type 2 (rt2) ooids, 3677.

The basal sequence recorded in Tizra 3-3 section (Fig. 3) contains late Asbian foraminifers and algae, but in addition, *Ademassa* and *Fascifolium* are recorded. Both of these taxa are more typically recorded in the Brigantian, although exceptionally, they first occur from the latest Asbian (Pille, 2008).

From the basal levels of the main bulk of limestones in the TZ2 Member, *Haplophragmina* and varied calcareous algae and problematica (*Neoprincipia*, *Sparaphralysia*, *Claracrusta*, *Falsocalcifolium* and *Richella*) are recorded. This suite of genera is typically recorded from the Brigantian (Vachard et al., 2016). The same suite of foraminifers and algae are recorded up to the upper part of the TZ3 Member, which also yields typical late Brigantian foraminifers (= lower part of the Serpukhovian sensu Cózar and Somerville, 2016), such as *Asteroarchaediscus baschkiricus*, *Climacammina* sp., *Howchinia gibba*, *Janischewskina delicata*, *Neoarchaediscus gregorii*, *Neoarchaediscus postrugosus*, *Planospirodiscus minimus* and *Tubispirodiscus* (= *Betpakodiscus* auct.) *attenuatus*.

3. Methodology

The carbonate microfacies were determined under the petrological microscope (on 180 large thin-sections, 50 x 80 mm), using the classification of Dunham (1962) in recognising the components and textures for the non-microbial limestones, whereas the terms employed by Sun and Wright (1989), Wright (1992), and Rodríguez-Martínez et al. (2010) were used in describing the microbial limestone facies. The abundance of grains, cement and matrix was visually estimated using the charts of Baccelle and Bosellini (1965). Skeletal and non-skeletal components are used (Supplementary material – Table S1) as defined by Flügel (2004). Skeletal and non-skeletal components are compared using Canonical Correspondence analysis (CCA). This ordination method is a linear combination of environmental variables versus well-known environmental parameters (Ramette, 2007). Owing to its results, the CCA is the most widely used gradient analysis technique for ecological studies (Palmer, 1993; ter Braak and Verdonschot, 1995). Identifying the index representative of bathymetry, it is possible to establish a stratigraphical gradient as defined by Cózar et al. (2019), similar to the previously defined gradient with Correspondence analysis (CA) for microbial mounds (Devuyst and Lees, 2001), or platform facies (Hennebert and Lees, 1991). The methodology published by Cózar et al. (2019) is followed herein, with the modifications explained in the supplementary material. The palaeoecological/environmental factors are stratigraphically analysed by means of the projection of the scores on the axes, and recalculated from 0 to 100. These indices allow to describe vertical evolution of the factors (Tables S1-S6). In order to decipher independent factors controlling the distribution of non-microbial and microbial facies, two CCA have been performed, for the non-microbial facies and the non-microbial facies with in situ generation of ooids, that apart from the energy, gives a predominant index (INM_1 and IOS_1 both representative of turbidity; Table S3). The CCA for the microbial facies gives four relevant indices (IM_1 = turbidity, IM_2 = energy, IM_3 = nutrients, IM_4 = chemical element

favouring calcification of skeletons; Table S4). The overall parameters of the succession are compared with another CCA, including all the samples, where the dominant factors are reduced to two indices (I_1 = energy/bathymetry and I_2 = turbidity; Table S5). A further CCA has been the focus on the samples yielding ooids, compared to the different parameters, and three main indices explain the variability (IO_1 = bathymetry, IO_2 = energy, IO_3 could not be identified; Table S6).

4. Carbonate facies description

Despite the relatively small size of the outcrop (c. 700 m long, southwest to northeast, 200 m wide, dipping 50-80^{o} east-southeast, and c. 100 m stratigraphic thickness; Fig. 2), several different carbonate facies and subfacies have been distinguished (Table 1). Limestones are predominantly pale grey to very pale grey, and with local brownish limestones in more argillaceous levels. The intraformational breccias (sensu Shinn et al., 1983; Miller, 1986) recognized in two levels as well as the shales are not described in detail.

facies	subfacies	cement and matrix	main components	biota	interpretation
grainstone	bioclastic	20-40% cement	crinoids, lithoclasts, ooids	abundant shallow and intermediate, moderate deep biota	shoals above FWWB
	peloidal	20-35% cement	>30% peloids, lithoclasts, crinoids, ooids	moderate shallow and intermediate, and poor deep biota	shoals above FWWB
	oolitic	25-40% cement	>25% ooids, lithoclasts, local peak of crinoids, quartz	moderate shallow and intermediate, and ppor deep biota	shoals above FWWB
grainstone-packstone	bioclastic	10-25% cement, 5-15% allomicrite	lithoclasts, ooids, crinoids	abundant shallow and intermediate, poor to moderate deep biota (cyanobacteria and bryozoans)	shoals with fluctuating conditions between the FWWB and SWB
	oolitic	10-20% cement, 10-25% allomicrite	>25% ooids, lithoclasts, crinoids	abundant shallow and intermediate, poor to moderate deep biota (cyanobacteria and bryozoans)	shoals with fluctuating conditions between the FWWB and SWB
packstone		15-25% allomicrite	lithoclasts, ooids, crinoids, fenestellids	abundant shallow and intermediate, poor to moderate deep biota (bryozoans)	tempestites
wackestone-mudstone	with packstone partings	10-40% allomicrite	quartz	abundant shallow and intermediate, moderate deep biota (bryozoan, ostracods, spicules)	open platform between the the FWWB and SWB
	wackestone	40-45% allomicrite	quartz, foraminifers, aoujgaliids, crinoids, fenestellids	moderate shallow, abundant intermediate, moderate deep biota (bryozoans, ostracods)	open platform below the SWB
	mudstone-wackestone	>60% allomicrite	quartz	poor shallow and intermediate, moderate deep biota	open platform below the SWB
clotted-micropeloidal	cementstone	10-45% cement, 15-50% automicrite	crinoids, brachiopods, fenestellids, foraminifers	poor shallow, moderate intermediate and deep fauna	open platform microbial buildups
	intraclastic-bioclastic	5-40% cement, 5-50% automicrite	intraclasts, crinoids, fenestellids	moderate shallow and deep fauna, moderate intermediate	open platform microbial buildups
	cement-supported	10-45% cement, 40-75% automicrite	fenestellids	poor shallow and intermediate, moderate deep biota	open platform microbial buildups
	matrix-supported	10-35% cement, 35-80% automicrite	local peaks of varied components, but none predominant	poor shallow and intermediate, abundant deep biota	open platform microbial buildups
	micritic	2-20% cement, 50-80% automicrite	local peaks of varied components, but none predominant	poor shallow and intermediate, abundant deep biota	open platform microbial buildups

Table 1. Main types of carbonate facies. Abbreviations: FWWB fair-weather wave-base; SWB storm wave-base

4.1. Grainstones

They are predominantly oolitic and bioclastic grainstones, and exceptionally peloidal (Figs. 4A–B). Bed thickness varies between 0.5 to 2 m, being thicker in the northern

outcrops. Lateral continuity of beds is limited to 50 to 100 m in the lower part of the succession (in the northern outcrops), whereas some beds in the uppermost part can be traced for several hundred metres, with some individual beds traceable throughout the entire 700 m of outcrop. Components are well sorted, with rare parallel lamination marked by the elongated bioclasts, with a low packing density, although the cement content varies from 20 to 40% in volume. Ooids usually developed thin cortices with few laminae, and mostly fit in the category of superficial ooids (Carozzi, 1957). Nuclei are more frequently bioclasts, peloids and more rarely quartz grains. When grainstones are bioclastic, most clasts are highly fragmented. The most common non-skeletal components are lithoclasts (micritic) of large size (several hundred microns in diameter) and more rarely smaller (less than 200 μm), locally peloids, muddy aggregates and quartz grains. The most common bioclasts are crinoids, whereas fenestellid bryozoans, foraminifers, brachiopods, ungdarellids (only represented by *Ungdarella*), dasycladales and aoujgaliids show local peaks, but they are not distributed in each sample. In some cases, grainstones are developed above and laterally to packstone textures, with a sharp boundary interpreted as erosive.

4.2 Grainstones-Packstones

These facies are rather similar to the previous type, but they contain between 5 to 15% of allomicrite (Figs. 4C–D), although cements are predominant (15-25%). Individual beds are usually 1 m thick, and they can be traced laterally for a few tens of metres. Skeletal and non-skeletal components are also similar, as well as rare parallel laminations. Half of the samples are mostly oolitic, and the other half bioclastic.

4.3. Packstones

This facies contains between 15 and 25% of allomicrite, and is poorly sorted, in cases with a bimodal size of clasts (Fig. 4E). Individual beds are usually 0.5 m thick, rarely amalgamated, to form limestone units up to 3 m with similar facies. Laterally, these beds can be traced for 100-200 m, and frequently pass to grainstone beds. Packing density is moderate to high. Cross-lamination and parallel lamination are observed, but rarely. The degree of fragmentation is variable, although generally high. Non-skeletal components are abundant, usually higher than 20% in volume, they are mostly composed of lithoclasts, ooids, quartz grains and muddy aggregate grains (in descending order of abundance) (Fig. 4F). Bioclastic content is more diverse than in the grainstone facies, although crinoids are the most abundant skeletal grains (up to 30-40% in volume), with common fenestellid bryozoans, brachiopods, aoujgaliids and ungdarellids. It is noteworthy, for a relative increase in the calcifoliids and foraminifers, as well as a decrease in dasycladales compared to the grainstones.

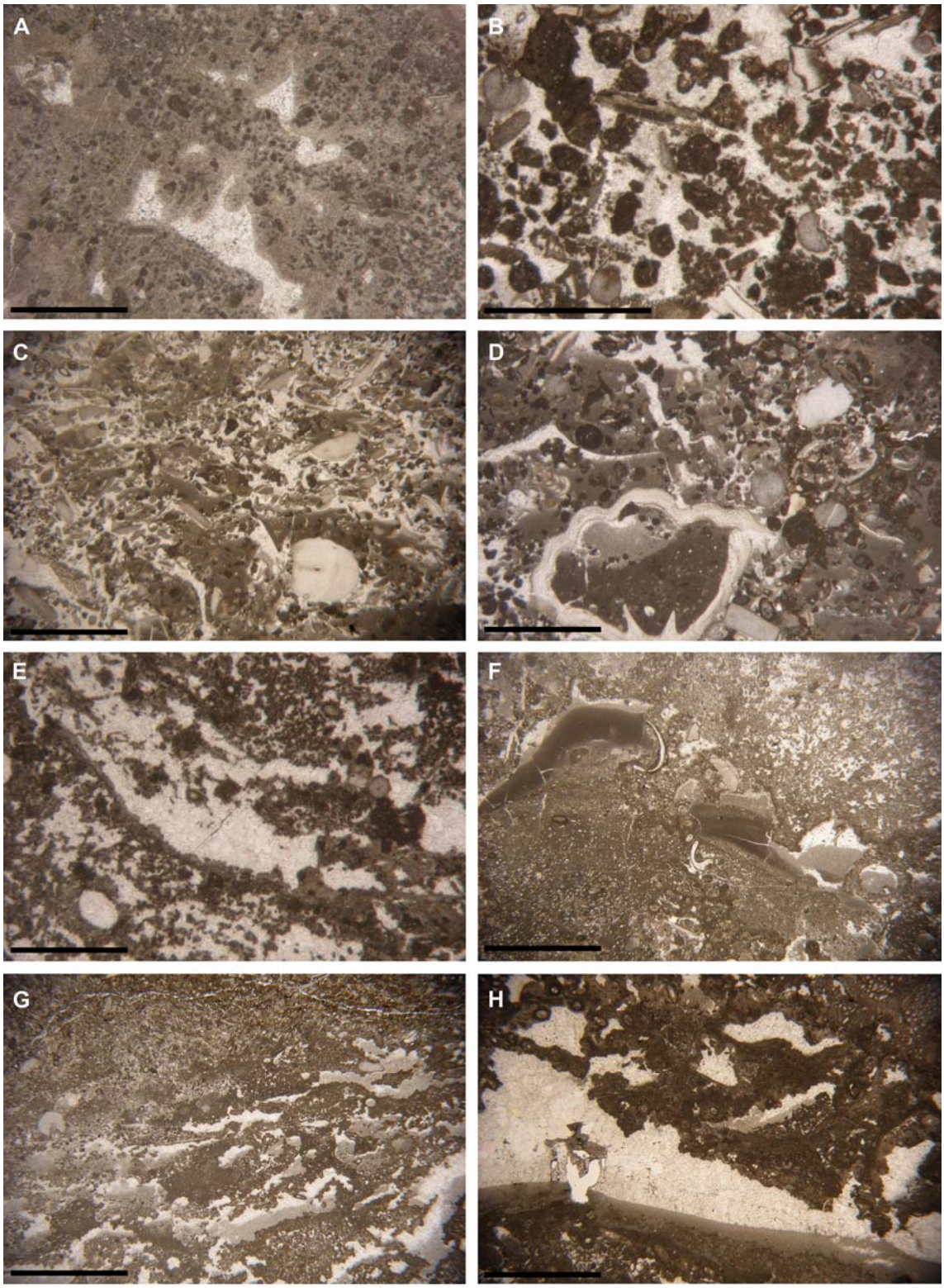

Fig. 5. Selected photomicrographs of microbial microfacies. Way-up to the upper part of the pictures. Scale bar for figs. A, B, D, E = 2 mm and for figs. C, F, G, H = 4 mm. A. Cementstone (to the left) passing to micropeloidal cement supported texture, most cement is typically RFC, 3675. B. Intraclastic cement-supported texture, note the pockets of dense micropeloidal automicrite, 3800. C. Bioclastic cement-supported (laterally cementstone) with common automicrites, 3639. D. Intraclastic-bioclastic matrix-supported, with common automicrites and allomicrite filling the base of the brachiopods (geopetal sediment), 3628. E. Micropeloidal cement-supported, 3654. F. Micropeloidal matrix-supported in the lower part passing into micropeloidal cement-supported (upper-right), in between, stromatactis cavities show polymuds, 3797. G. Micropeloidal matrix-supported with common stromatactis cavities with a single generation of internal micrite infilling passing into a packstone, 3799. H. Micropeloidal matrix-supported with fenestellids and encrusting bryozoans associated to the top of the cavities with geopetal micrite at the base, 3791.

4.4. Wackestones-mudstones

These are a minority facies in the sections, and usually, they occur in close relationship with shales and the microbial facies (Fig. 4G). Bed thickness is 0.5 to 1 m, stacked in intervals up to 2.5 m thick. Laterally, these beds are rather impersistent, and only extends for a few tens of metres. Bioclasts are partly broken, with subtle parallel orientations of tiny ostracods or brachiopods (Fig. 4H). The percentage of bioclasts is lower than 50%, and mostly composed of aoujgaliids, fenestellid bryozoans, ostracods, and also common silt-size quartz grains.

4.5. Clotted-micropeloidal limestones

This facies contains clotted and micritic fabrics, and rarely cementstones. Stratification surfaces are rarely observed within these limestones, and they are usually limited by the other previous lithologies. Thus, in the northern outcrops, beds vary commonly from 1 to 5 m thick, but can be up to 8-9 m. The southern outcrop also contains relatively thin beds, 2 to 5 m thick, but the overall thickness increases, up to 15-30 m, and even as high as 50 m in Tizra 3 section without any apparent bedding planes. In the southern part, beds can be traced trough the blocks separated by faults, whereas in the northern part, they have metric to decametric lateral extension. Clotted fabrics are varied, including micropeloidal matrix- and cement-supported, as well as bioclastic-intraclastic (with a progressive increase in the amount of cement). Generally, the larger amount of cement also corresponds to a higher bioclastic content. Most cements are granular, blocky and equant sparite, and radiaxial fibrous calcite (RFC) cements are comparatively scarce, but rims of RFC around clasts and vugs are common. The term cementstone is preserved for those facies with a predominance of RFC cements (Fig. 5A), whereas other facies with common cements are considered cement-supported (Figs. 5B–C, E). Large stromatactis cavities are scarce (Figs. 5F, H), and they mostly occur in the southern sections (Tizra 3-1 and Tizra 3), whereas smaller fenestrae are commonly distributed in all five logged sections (Figs. 5E, G). Matrix-supported fabrics contain common bioclasts, intraclasts, as well as automicrites, and locally, allomicrites (Figs. 5D, F–H). The most abundant bioclasts are fenestellid bryozoans, crinoids, brachiopods and encrusting bryozoans, and secondarily, calcifoliids (mostly *Fasciella*), cyanobacteria (*Girvanella* and *Ortonella*), thin-shelled ostracods, sponge spicules, foraminifers, and aphralysiaceans (possibly another cyanobacteria). Other bioclasts are much rarer, but diverse, including dasycladales and rare solitary rugose corals. On the other hand, quartz grains are common, as well as ooids, which are clearly embedded in a micropeloidal matrix, and rarely, infilling cavities. The variations between the different fabrics do not follow any identifiable pattern, and they occur commonly laterally, as well as stratigraphically above and below (Fig. 3). Boundaries between fabrics are transitional, and sharp contacts are only present when non-microbial facies occur. Domical, stromatolitic and oncolitic growths are rare, but present. Firmgrounds are also rare. Processes of micritization and borings/microborings are commonly recorded. Within the facies including “intraclasts”, there are two samples

with large micropeloidal intraclasts, with more abundant iron oxides between the intraclasts, but there is no mixture of clasts, nor other hydrodynamic sorting nor orientation.

5. Ooid types

The concept of ooids is not free of controversy, as well as their formation (Harris et al., 2019). Older classifications presupposed a biological origin for oncoids and a non-biological control for the formation of ooids (e.g., Davies et al., 1978; Peryt, 1983). However, after recognizing that ooid formation required microbial mediation (e.g., Duguid et al., 2010; Diaz et al., 2015), genetic classifications were abandoned, and descriptive terms prevailed (e.g., Ritcher, 1983; Steinhoff and Strohmenger, 1996; Flügel, 2004). Nevertheless, there is still a paradigm whereby elongated ooids form due to the elongated shape of the nucleus and usually do not have perfectly symmetrical and concentric cortices. In such cases, they are classified as oncoids, aggregates or simply coated grains, whereas most current experiments are based on typical rounded concentric coated grains or slightly egg-shaped ooids (e.g., Rankey et al., 2006; Trower et al., 2017; Harris et al., 2019).

	roundness	fabric	cortex	cortex thickness	nucleus	diameter	
Regular type 1	rounded	radial	1-2 laminae	25-75 µm	peloids, small bioclastic fragments	< 300 µm	Fig. 6A
Regular type 2	rounded	radial and tangential	1-2 laminae	25-100 µm	bioclasts, lithoclasts	300 to 600 µm	Fig. 6B
Regular type 3	rounded	radial and tangential	>3 laminae	50 and 200 µm	bioclasts, lithoclasts, quartz grains	400 to 900 µm	Fig. 6C
Irregular type 1	subrounded	radial and tangential	1-2 laminae	25-75 µm	brachiopods, molluscs, trilobites, ostracods	300 to 900 µm	Fig. 6D
Irregular type 2	elongated and irregular	tangential	1 to 4 laminae	50-200 µm	large elongated bioclasts, rarely lithoclasts	400 to 1700 µm	Fig. 6E
Irregular type 3 or compound ooids	irregular	tangential	1-2 laminae	50-100 µm	ooids	>600 µm	Fig. 6F

Table 2. Main features of ooids

Ooids recorded in Tizra samples can be classified based on their roundness, cortices and nuclei. The first subdivision is based on roundness, because there are regular (rounded to egg-shaped) and irregular ooids (elongated or with irregular forms) (Table 2). Cortices can be poorly developed, with only one or two laminae, or have a much higher number of laminae. The type of nucleus has a strong influence on the resulting growth and readily conditions the final form, depending on if it were small peloids or mud peloids, small fragmented bioclasts (in such cases termed pseudo-oolites, sensu Carozzi, 1960), quartz grains, large lithoclasts, large elongated or irregular fragments of bioclasts (e.g., brachiopods, crinoids, trilobites), or even an amalgamation of previous ooids. According to the definition of Carozzi (1957), most ooids in Tizra are superficial, because the cortices are generally less than half of the total diameter. The combination

of the previous parameters gives us six main types of ooids (Table 2; Fig. 6): Regular type 1, Regular type 2, Regular type 3, Irregular type 1, Irregular type 2, Irregular type 3 (or compound ooids).

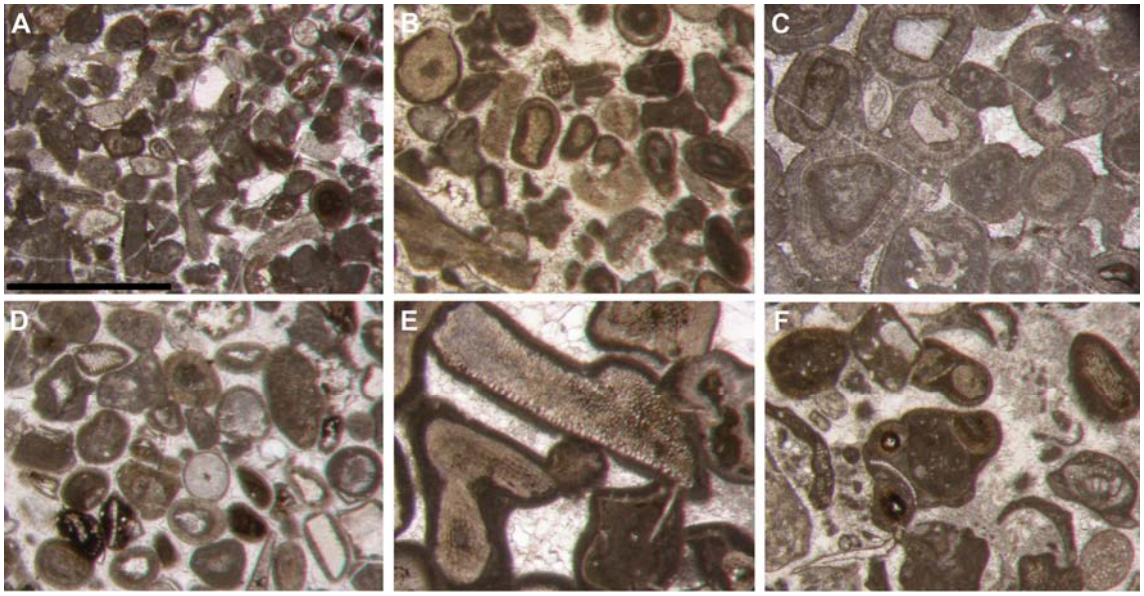

Fig. 6. Main types of ooids (scale bar = 1 mm). A. Regular type 1 with thin tangential cortices, 3742. B. Regular type 2 with thin tangential cortices, 3790. C. Regular type 3 with thick radial cortices, 3984. D. Irregular type 1, note that half of the ooids are regular type 2 also, radial cortices, 3682. E. Irregular type 2, tangential cortices, 3741. F. Irregular type 3, (compound ooids) with tangential cortices, 3661.

In some cases, irregular types 1 and 2 do not present concentric laminae in the cortex (Figs. 6D–E), which, according to some authors, might suggest their inclusion as oncoids or aggregates, but it is interpreted herein, that the absence of parts of the laminae is a result of erosion, which usually also affects the exposed part of the nucleus. Compared to the classification by Steinhoff and Strohmenger (1996), our regular types 1 to 3 correspond to the types 1- to 3-ooids (respectively), whereas the irregular type 1 might correspond to the type 2-aggregates, and the irregular type 3 with the type 1-aggregates, although as mentioned above, we have observed or inferred completely concentric and continuous laminae. We do not find an equivalence for the irregular type 2. In general, there is a direct relationship between the diameter of the ooids and the thickness of the cortices (Fig. 7A).

If the types of ooids are compared with the facies, the predominant parameter is, assuming that ooids could not be generated in the microbial facies, the transport capacity of the different types of ooids. The result is that, the small regular type 1, type 2 and irregular type 1 ooids are commonly recorded in the grainstone facies, where they were generated, as well as in the microbial facies, where they more commonly accumulated due to their small size and capability to be longer transported into the deepest water facies of the platform (Fig. 7B). If samples yielding in situ generation of ooids are compared, the results are more marked, highlighting that the irregular types 2 and 3 are mainly associated with the grainstone-packstone textures (Fig. 7C). This fact suggests that the more irregular energy levels and quiet water in grainstone-packstone likely reached higher values, so as to generate larger ooids arising from a larger and

heavier nucleus, but they were more difficult to transport. Regular and constant energy levels in grainstones induced higher abrasion rates, and when the moderate size was achieved as the equilibrium size (Trower et al., 2017), larger regular type 3 ooids rarely formed, as well as the relatively low energy level did not allow the constant motion of the large bioclasts necessary to generate the irregular type 2 ooids and large compound ooids. This fact agrees with the interpretation of Freeman (1962) for the large and asymmetrical ooids.

In addition, there is a predominant radial fabric in grainstones with regular type 2, irregular type 1 and regular type 3 ooids, where the tangential fabrics shift to the grainstone-packstone facies (Fig. 7D). We have not observed a direct relationship between the fabrics of the cortices with the size of the ooids, as proposed by Heller et al. (1980), and in contrast, many large regular type 3 ooids (e.g., 700-800 μm) show preferential radial fabrics (Fig. 6C).

6. Facies interpretation

Grainstones and grainstones-packstones developed mainly in intertidal to subtidal conditions, locally with little micrite concentration between the bioclasts and ooids. These beds show all the typical features of shoals with high energy (Allen, 1980; Harris et al., 2019). In grainstone facies, although broken and regenerated ooids are observed (Figs. 6D, 8A), they present generally a good preservation of shape and cortices, only affected by local abrasion or bioerosion, features which are compatible with the environments. However, in the grainstone-packstone facies, half of the samples contain transported ooids (Fig. 8B), whereas the other half shows perfectly preserved specimens (Figs. 4D, 8A), which led us to interpret the latter as having been generated in situ.

The packstone facies, however, contain characteristics of storms, in concentrating bioclasts of the platform, as well as common ooids from non-lithified substrates, cross- and parallel laminations, bimodal sorting, etc. All the ooids in the packstone facies present strong erosion of the cortices, even breakages or facets (Fig. 8C), which are interpreted as having been transported during storms. Rare wackestones and mudstones are interpreted as the calm background, low-energy sedimentation on the platform, together with the shales, that accumulated in the deepest-water setting below the storm wave base (SWB). Some lags show a marked concentration of ooids in partings with parallel orientation of the elongated axes (Fig. 4H).

Clotted and micropeloidal facies are considered as microbial boundstones. These types of boundstones are precipitated in shallow and deep water conditions (Camoin et al., 2006). Internal fabrics do not show any apparent trend, and do not allow to infer variations of the boundstones (Fig. 3). Rare intraformational breccias are recorded, but clear episodes of emersion or energy levels were not observed. The dominant morphologies of the boundstones are nearly stratiform, with lumpy reliefs, which seem to be the result of coalesced mounds growing mostly laterally from the north to the

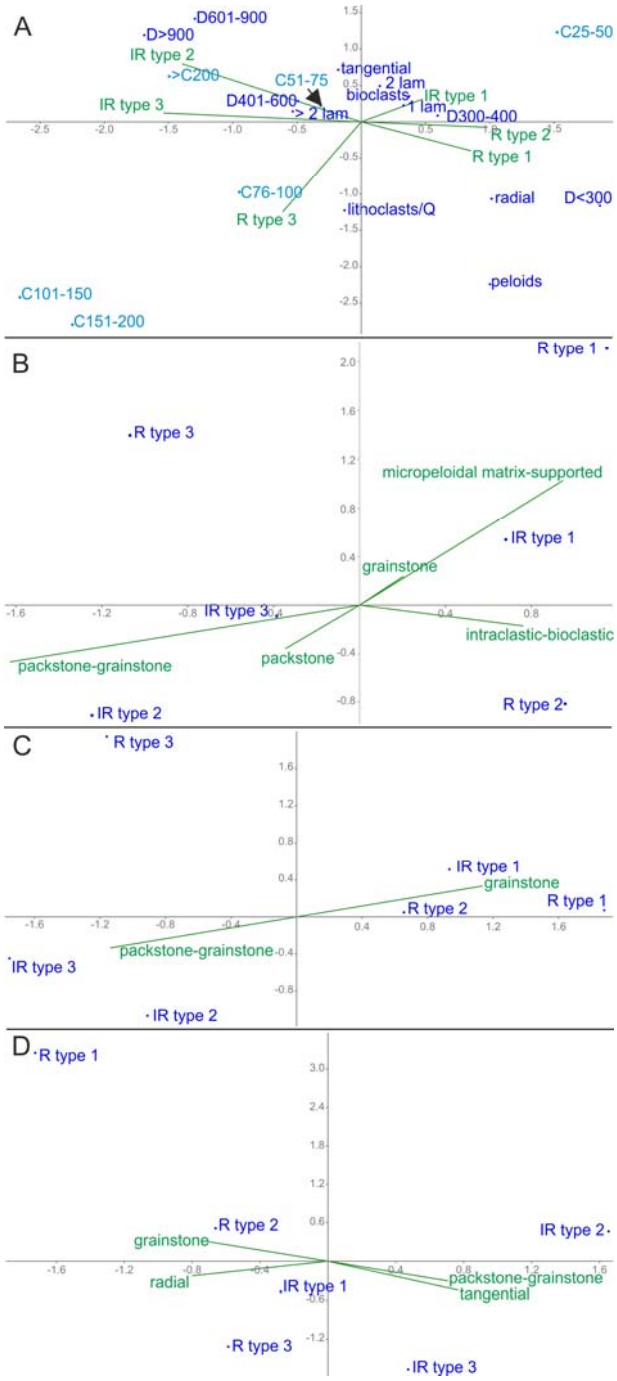

Fig. 7. Triplot CCA graphics. A. types of ooids versus parameters and nuclei of the ooids. B. Types of ooids versus predominant facies. C. Types of ooids versus facies of in situ generation. D. Types of ooids versus facies (in situ) and cortex fabric. R: regular, IR: irregular, D: diameter, C: cortex, lam: laminae.

south of the area. Vertical accretion of some mounds is significant, but does not represent the predominant tendency in the platform. There are small dome-shaped mounds recorded interbedded within the shallow water grainstones and packstones. The common ooids recorded in microbial facies are always well preserved (Figs. 8D–I) and it is assumed that such ooids mostly arrived by floating or were gravity-driven. The highest accumulation of ooids in clotted/micropeloidal facies corresponds to bioclastic-intraclastic subfacies, which are related to periods of higher energy in the mound (Cózar

et al., 2019; see also index *IM*$_2$ later), and ooids also occur filling cavities (Figs. 8F–G). However, the most striking ooids are well-preserved regular type 3, in the middle of micropeloids (Figs. 8H–I), although they also occur in patches, and usually, are associated with intraclasts and bioclasts, which suggest elevated energy levels for the mounds. Using these criteria, only 26 samples out of a total of 67 yielding ooids in the different facies are interpreted to be representative of their place of generation (Fig. 3), whereas the rest of the samples are interpreted as places of accumulation (see also columns in situ/transported in supplementary Table S2).

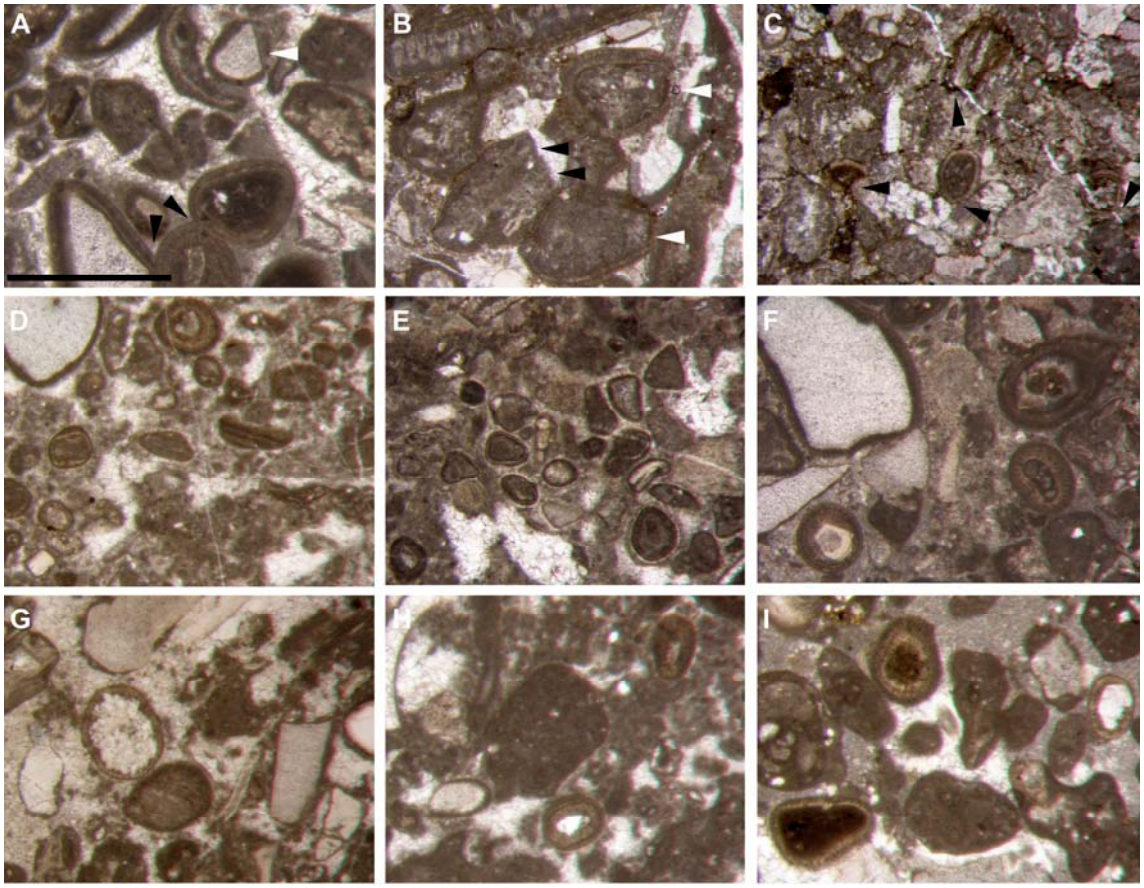

Fig. 8. Types of ooid preservation (scale bar = 1 mm). A. Pressure dissolution by compaction in regular type 3 and irregular types 1 and 2 ooids (black arrows) formed in situ in a grainstone-packstone; in some cases, erosion led to the loss of laminae which start rapidly to be regenerated (white arrow), 3662. B. Transported regular type 3 and irregular type 2 ooids with erosion facets (black arrows) and loss of laminae (white arrows) in a grainstone-packstone, 3684. C. Transported regular types 1 and 2 ooids with erosion facets (arrows) between lithoclasts in a densely packed packstone, 3667. D. Well-preserved regular types 1 and 2 ooids in micropeloidal matrix-supported subfacies with small fenestrae, 3712. E. Well-preserved rather superficial regular type 2 ooids in a microbial intraclastic subfacies, 3702. F. Well-preserved regular type 3 and irregular type 2 ooids filling a cavity with other bioclasts and intraclasts in micropeloidal matrix-supported-micrite subfacies, 3663. G. Well-preserved regular type 2 ooids filling a cavity in a microbial intraclastic subfacies, 3656. H. Well-preserved regular type 3 ooids in the middle of a micropeloidal matrix-supported subfacies, note the occurrence of large intraclasts and molluscs, 3665. I. Well-preserved regular types 2 and 3 ooids in automicrites with common intraclasts, 3798.

The general succession is interpreted as having been deposited on a shallow-water platform, developed above the SWB and with frequent intervals above the fair-weather wave base (FWWB). Hemipelagic or pelagic environments seem not to be present, although the southern extension of the limestones is abruptly interrupted by a fault (Fig. 2). Emersion surfaces and subaerial features have not been recognized, and thus, the platform was always submerged. There is diversity in the bioclasts, including

stenohaline fauna living in open marine conditions, with normal temperatures, constituting typical photozoan carbonates, also for the microbial facies, rich in dasycladale algae. The relative abundance of grainstones (shoals), packstones (tempestites) and microbial limestones (boundstones) suggest an overall inclination of the shelf towards the southern outcrops (Fig. 3), where the deeper water facies are thicker and less influenced by storms.

7. Ecological controls on the development of non-microbial carbonates

The Dunham (1962) depositional textural scheme led to a genetic classification, mostly as a representation of the different energy levels. The grainstone and packstone facies are both of high energy, and the distinguishing controlling factor between them is the more-or-less stable high-energy condition in grainstones which allows the winnowing of the micrite. The CCA for the non-microbial carbonates, assumed this energy control, gives only a marked index controlling 85.9% of the distribution, which is interpreted as the degree of turbidity (Table S3). This gradient is in fact a measure of a more constant (waves/tides) or episodic (storms) energy on the platform, allowing for the winnowing of micrite. In this distribution, all the samples above $INM_1 = 50$ correspond to tempestites with common muddy transported material, whereas those below 50 correspond to sedimentation in the shoals or incipient bars. The influence of storms in the southern sections is less important, and they are more frequent in the northern sections (Fig. 9).

If the same comparison is used for the facies with in situ formation of ooids, the same trend is observed from clearer water facies to those yielding allomicrite, the latter being situated at value 100 also (Table S4, index ISO_1). Grainstone levels are closely related to the regular types 1 and 2, and irregular type 1 ooids, and are associated with levels rich in shallow-water and clean-water adapted biota, principally molluscs, foraminifers and dasycladale algae. In contrast, the regular type 3, and irregular types 2 and 3, are located in positions closer to the grainstone-packstone, with similar values as the ungdarellids, trilobites, crinoids, calcifoliids, aoujgaliids, biota which could have inhabited intermediate water depths or turbid settings (Cózar et al., 2019). The highest values are shown by cyanobacteria, brachiopods, aphralysiaceans, palaeoberesellids, bryozoans, red algae and ostracods. Except for the brachiopods, it is an assemblage typical of deep and turbid waters (Cózar et al., 2019). This parameter resulting from the samples with ooids is also an indirect measure of the turbidity of the environment that coincides with levels of lower energy or less constant energy in the grainstones-packstones.

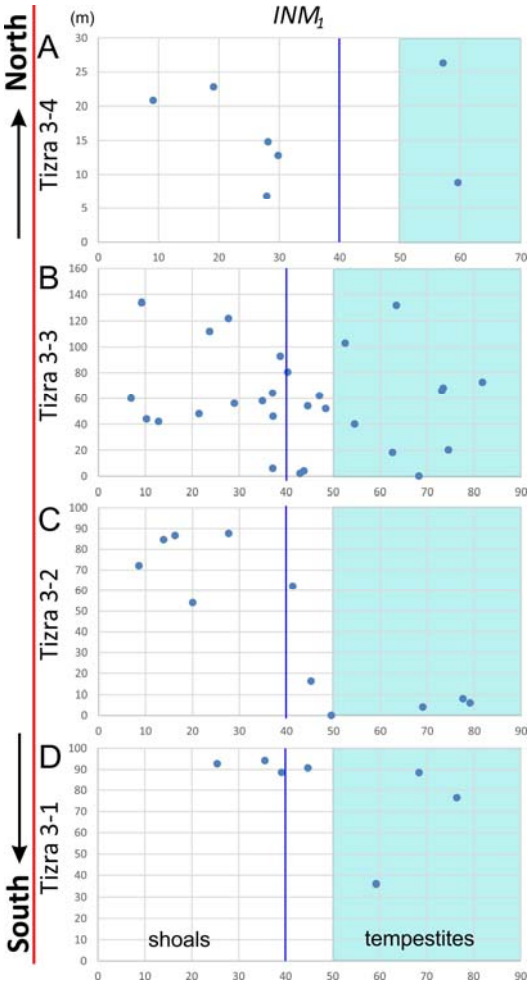

Fig. 9. Representation of the thickness of each section (in axis y, in metres), and the non-microbial INM_1 values for each sample on axis x (turbitidy).

8. Ecological controls on the development of microbial carbonates

Some of the main inhibiting factors for the growth of the Carboniferous microbial mounds are the high energy levels and massive input of clastic material (Lees and Miller, 1995; Leinfelder et al., 1996). The CCA shows two main parameters controlling the distribution of components and textures (IM_1 and IM_2), and two secondary indices (IM_3 and IM_4), with a certain weighting (Fig. 10; Table S4).

8.1. IM_1 *gradient*

Turbidity (as a measure of the clay and silt content in suspension), is interpreted to be the dominant factor IM_1 (48.36%). It is noteworthy, for the low values for most components (Table S4), even considering the dasycladales as a marker for the quantification of light penetration, with its value of 22.81, which is a result of the low turbidity environments during the growth of the microbial communities (Figs. 10A–D). Only the palaeoberesellids and, mostly the common occurrence of quartz grains, seems to be a result of more turbid conditions. More turbid levels (with values >22) are located at the base or top of the mounds in direct relationship with the immediately overlying or

underlying shales. This is not an unexpected result, because, as demonstrated by Cózar et al. (2019), the deeper-water microbial mounds in the Carboniferous of Montagne Noire (southern France) developed in less turbid settings than the shallower-water stratiform microbial limestones.

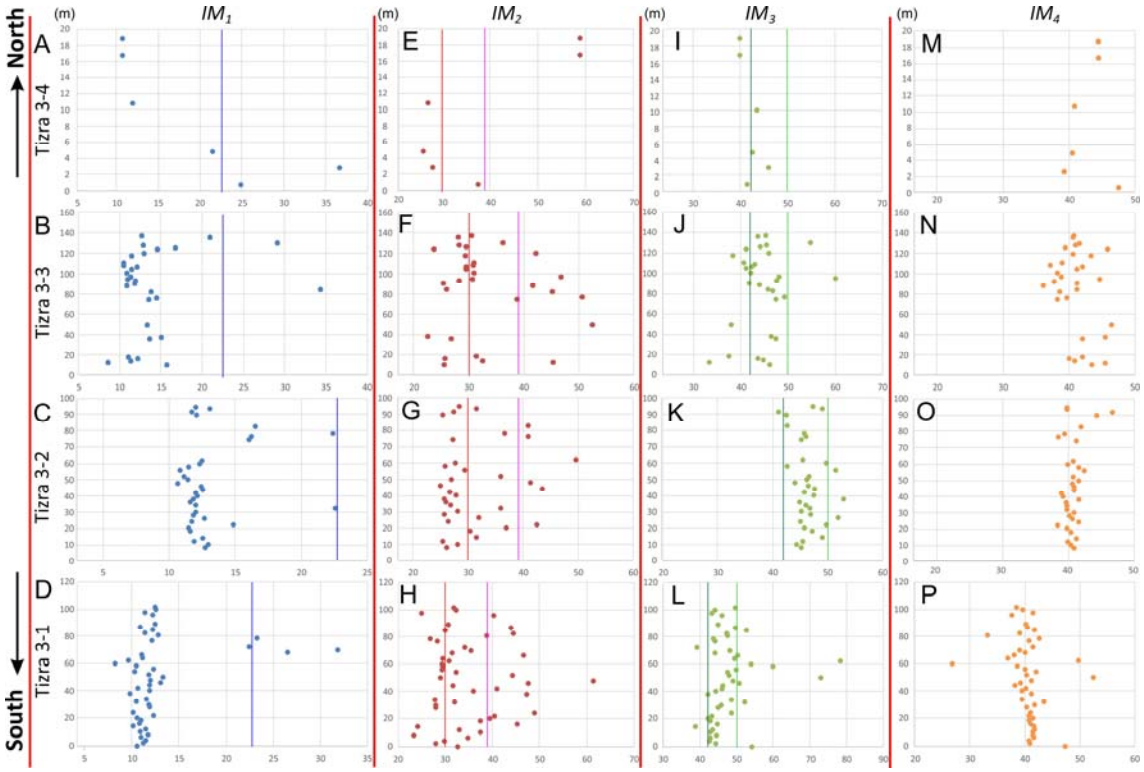

Fig. 10. Representation of the thickness of each section (in axis y, in metres), and the microbial IM_1 index (A-D, turbidity; values less than 23 correspond to euphotic conditions); IM_2 (E-H, energy; values less than 30 are below the micritic facies, in the lowest energy levels; values greater than 39 are those of more higher energy due to the occurrence of cements), IM_3 (I-L, nutrients; values higher than 50 yield those levels with more nutrients, and those below 42 with less nutrients) and IM_4 (M-P), values for each sample on axis x.

8.2. IM_2 *gradient*

The second index, IM_2 (29.21 %), seems to be related with currents affecting the mounds (Figs. 10E–H; Table S4). In the lower levels of the gradient, the sponge spicules, *Terebella*-like tubes, agglutinated foraminifers and thin-shelled ostracods occur associated with the automicrites. These components are typically recorded in calm/deep water environments (Cózar et al., 2019). Calcifoliids, which also occur, have a wider ecological tolerance and thus, they can occur in a variety of environments. Unlike ooids, the appearance of oncoids is apparently controlled only by the periodic need of energy for turning, rolling and displacement for the growth of the successive cyanobacteria cortices (Flügel, 2004). However, they can be transported from shallower water settings, even being frequent in slope setting of similar ages (Cózar et al., 2003; and references therein), as well as for more recent rhodolites (Ginsburg and Bosellini, 1973; Bosence, 1983). In the opposite extreme of the gradient, the intraclasts are

located, together with ungdarellids, aoujgaliids, ooids, crinoids and brachiopods, which are associated to tolerate higher energy conditions, and the intraclasts, themselves, need energy for their formation. In addition, these components are commonly present in bioclastic textures and associated to a higher percentage in cement. The abundance of bioclasts also suggests a certain energy to contribute to the environment nutrients, which are more abundant in the intraclastic-bioclastic facies, as well as those rich in cement. The value of 30 marks the boundary of the automicrites, and above 40, textures richer in cements occur (micropeloidal cement-supported and cementstone), and thus, with more constant currents in the environment to winnow the micrite.

Other bioclasts that should intuitively be considered typical of moderate or shallow-water depths, such as the red algae, and in particular the dasycladales, are recorded in the lower part of this gradient (low energy), which might contradict a bathymetric correspondence. The state of preservation of the dasycladales is generally good, suggesting rather low-energy conditions or only sporadic, forming autochthonous and paraautochthonous assemblages. However, as discussed by Cózar et al. (2018), it is not clear if the Mississippian dasycladales could be used universally as markers of <10-15 m depths, as is the case for most of the modern dasycladales (Berger and Kaever, 1992; Graham and Wilcox, 2000), and they might have tolerated slightly deeper-water environments. Similar concerns about the ecological parameters controlling the distribution of Mississippian algae compared with modern algae have been documented previously (Wray, 1977; Bourque et al., 1995). The preserved profile of the platform (Fig. 2) suggests that the bathymetric difference between the northern shoals and the southern mounds in the lower part of the succession could be estimated to be about 20-30 m. Thus, comparing with the dasycladale distribution in Mississippian mounds of France (Cózar et al., 2018, 2019), these algae in the Tizra Formation could be present in any part of the platform, and this bathymetric difference does not seem to be sufficient to prevent their occurrence, even in the deeper part of the mounds of Tizra.

8.3. IM_3 *gradient*

The index IM_3 (7.57%) contains the Algospongia, oncoids, ooids, sponge spicules, aphralysiaceans, *Terebella*-like tubes and quartz grains in the lower values, whereas the foraminifers, brachiopods, ostracods, crinoids and bryozoans are situated in the other extreme (Table S4). This index IM_3 is interpreted to be related with the amount of nutrients, showing predominantly, the non-dependent components and some problematic algae in the low values, and most invertebrates and protozoa in the higher values. Owing to the small size of the platform, and taking into consideration the individual values for the samples, there is no observed trend in the mounds of the different sections, although variations occur (Figs. 10I–L), but the peaks of each section do not coincide stratigraphically with peaks in other sections. It can be only generalized that values of about 50 or even higher (more nutrients) are usually associated with the more micritic textures in the boundstones, whereas the other four microbial textures result with values between 35 and 47. The lowest value, between 37 and 43, are more

associated with textures rich in cements (cementstone, as well as micropeloidal cement-supported), but also present in other textures.

8.4. IM_4 *gradient*

The index *IM₄* has also very little influence on the distribution of components (6.29%) in the mounds. In the lower values of this index are apharalysiaceans, cyanobacteria, calcifoliids, ooids, red algae, foraminifers and brachiopods (Table S4). These components are characterized by being rather robust and having stable biomineralizations of their respective walls. They constitute a group where only stronger diagenesis affects their structures and microstructures, being usually very well preserved. In contrast, in the opposite extreme, dasycladales, ungdarellids, palaeoberesellids, trepostomate/encrusting bryozoans, sponge spicules, ostracods, and molluscs are recorded. In the Algospongia, except for the more stable walls of the calcifoliids, the wall in the other families are commonly partly recrystallized, and their original wall nature is not well known yet (Vachard and Cózar, 2010). Recrystallization of the thin-walled ostracods is also common, as well as the typical preservation of sponge spicules (as calcite molds), molluscs and dasycladales only as recrystallizations and cements. In between those bioclasts, statistical artifacts occur for non-dependant components of carbonate precipitation, such as the quartz grains. This *IM₄* is interpreted as the result of a chemical variation in the sea water. It could be proposed as a lower percentage in magnesium in the more stable shells, however the varied types of walls, structures, microstructures, and compositions of the involved bioclasts, do not allow to identify unquestionably the precise chemical element.

The vertical gradient for *IM₄* shows more uniform values for mounds of the southern sections, except for the upper part of the succession, where some fluctuations are observed (Figs. 10M–P). In contrast, constant fluctuations are observed in the northern mounds. This fact might be related to shallower water environmental conditions in the northern sections (as was observed for the facies variations), close to the source of chemical elements by means of the deltaic deposits.

9. Discussion

According to the individual ecological factors for each type of lithology, turbidity and energy are the dominant ecological factors in the distributions of components and facies, although they do not give us the overall controls on the morphology and architecture of the platform. Other intervening factors can also be discussed for the overall architecture of the platform.

9.1. Syn-sedimentary tectonics and accommodation space

The syn-sedimentary faults allowed the growth of microbial mounds to the south, generating slightly deeper-water and calmer conditions, and the mounds become progressively thicker southwards, mostly in sequence S1. The orientation of the small

platform is clearly north-south, where the influence of the landward terrigenous influx is marked by the thinning of the carbonate succession and thickening of shales to the north. It must be noted that the shales corresponding to the underlying TZ1 Member were interpreted as deltaic facies (Berkhli et al., 2001), whereas more open marine shales are interpreted herein for the shales in TZ2 Member.

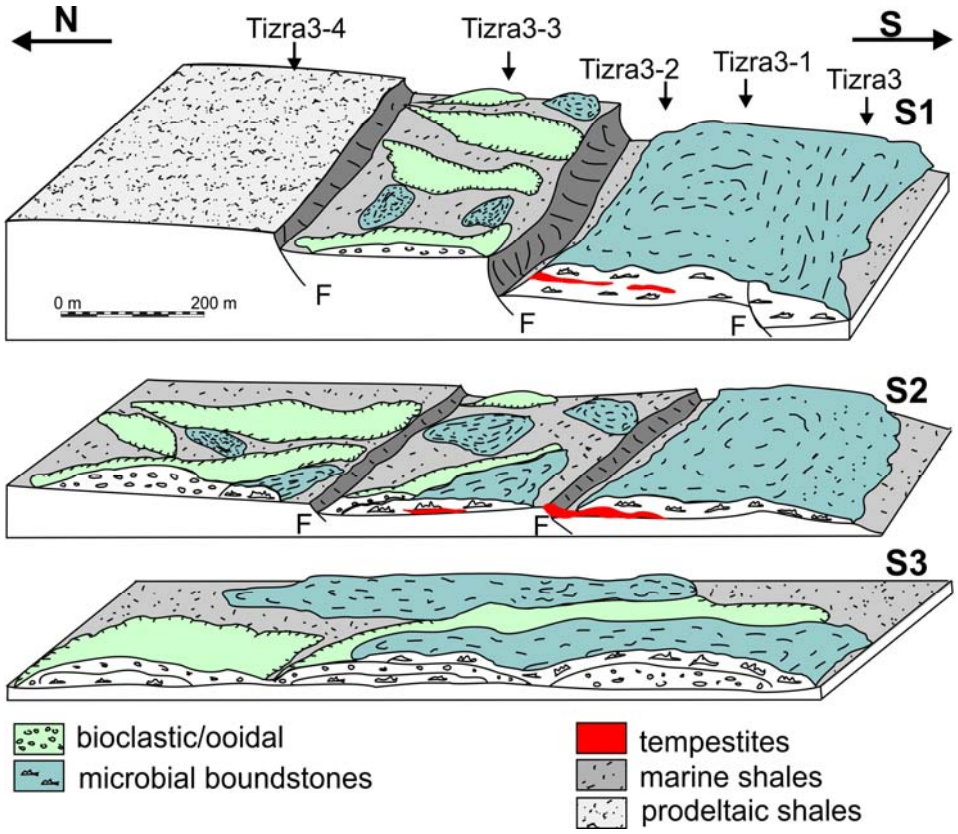

Fig. 11. Schematic representation of facies distribution across the platform during the deposition of sequences S1 to S3 and involvement of syn-sedimentary faults (F). Scale is approximate.

The large shoal in S1 sequence (Tizra 3-3 section), could be attributed to those developed in a typical transgressive sequence, with the ooids and bioclasts forming in the shallower water setting under intertidal conditions, and its lateral extension is limited by the deeper water subtidal conditions favoured by the dip of the shelf generated by the syn-sedimentary faults. These faults favoured higher accommodation space for the growth by accretion of large mounds with smooth relief (Figs. 2, 11), although, as can be seen from the shoal at the base of the sequence (e.g., in Tizra 3-2 section), there is also a seaward lateral growth of the mounds. Within this sequence 1, there is an increase in thickness seawards (Table 3), which coincides with the part of the succession affected by the movement of the syn-sedimentary faults (Fig. 2). Similar shoals with sparse mounds in deeper water conditions were described by Dilliar et al. (2010), although the syn-sedimentary faults described by those authors separated the inner platform from the gravity-driven deposits in a marked slope, whereas internal faults within the inner platform were not described. A typical slope is not recognized in Tizra (Fig. 2), only very localized levels with breccias (with microbial pebbles), which

could be attributed to a slope setting, and thus to debris flows, but also to strong tempestites in the distal part of the shaley platform. According to Dilliar et al. (2010), their microbial mounds developed in a calm setting between the shoals, which could be the case for the lower part of S1 in Tizra 3-3 section, as well as for S2 and S3 in Tizra 3-4 section (Fig. 11). The S2 sequence also shows a predominance of microbial facies to the south and more bioclastic facies in the north, and thickness variation depends on the section (Table 3).

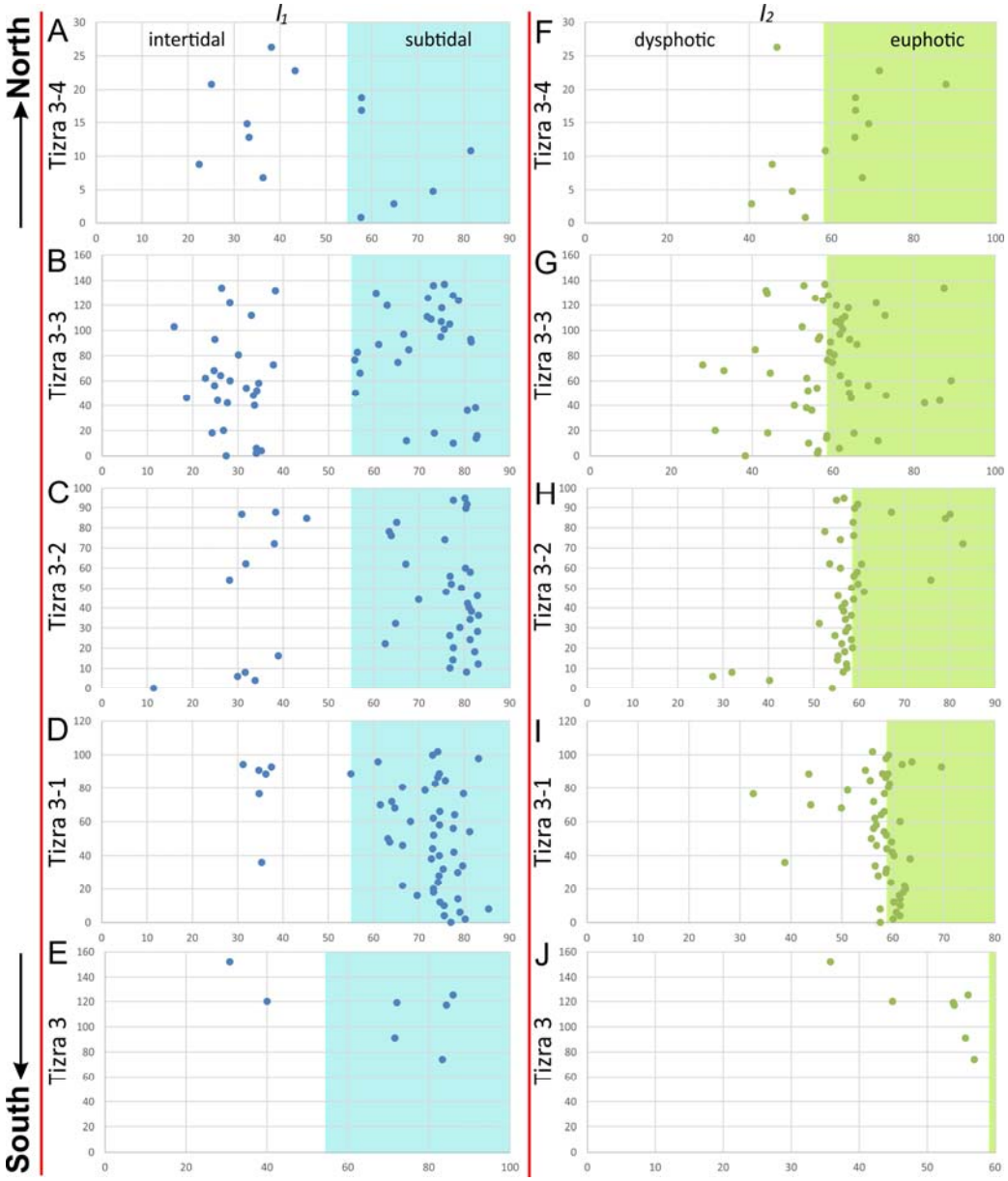

Fig. 12. Representation of the thickness of each section (in axis y, in metres), and the I_1 index (A-E, energy), and I_2 (F-J, turbidity) values for each sample on axis x.

The younger S3 sequence is distinct, and developed thick bioclastic grainstone deposits to the south, which pass northward into oolitic grainstone. The similarity in thickness and facies for S3 suggests that (Table 3), first, the shelf was mostly levelled, and second, that the two main faults observed in the field intersecting the sequence

acted mostly in post-sedimentary phases, and the displacements of beds did not modify the main lithologies, thicknesses and environmental conditions (Figs. 2–3). This seems to be also valid for S2, although in this case, a certain thickening of the sequence is observed juxtaposed to the faults, suggesting still a syn-sedimentary behaviour for them. These deposits of S3 can be compared to those described in the lower part of the Point Peak Member by Lehrman et al. (2020), where the reduced microbial growths and with a predominant lateral coalescent structures were interpreted as a low accommodation space within the inner platform.

	Tizra 3-4	Tizra 3-3	Tizra 3-2	Tizra 3-1	Tizra 3
S1	—	63	71	76	63
S2	10.5	26	11.5	11.5	28
S3	20	22	18	17	15
S1/1	—	11.3	13.7	16.6	—
S1/2	—	15.6	5.9	6.	—
S1/3	—	5.3	11.5	14.1	—
S1/4	—	12.5	11.7	13.6	—
S1/5	—	11.4	10.5	10	—
S1/6	—	10.5	18.7	15.9	—
S2/7	8.8	8.4	6.6	10.2	—
S3/8	5.6	9.8	9.1	8.3	—
S3/9	6.5	11.3	8.4	7.2	—
S3/10	5.5	3.5	—	—	—

Table 3. Thickness variation of the sequences and cycles (in metres)

9.2. Energy/bathymetry

Two significant factors for controlling the distribution of facies and components have been identified, named as I_1 (controlling the 55.08%) and I_2 (27.58%) (Table S5). The I_1 index contains the lithoclasts as value 0, and ooids, allomicrite, ungdarellids, aoujgaliids and palaeoberesellids with low values, whereas in the other extreme, intraclasts, automicrites, sponge spicules, agglutinated foraminifers and *Terebella*-like tubes occur. This index is a gradient of the energy on the platform, with higher values trending to 0, and the components characteristic of calm environments are close to 100. Indirectly, except for some local tempestites (e.g., sample Pc2756, Fig. 3), these I_1 values give also a quantification of the bathymetry of the platform, with the shallow-water conditions in low values, and the deeper-water settings in higher values. The vertical ecological gradient for I_1 in the sections shows rapid variations between calm/deep and more energetic/shallower environments (Figs. 12A–E). Taking into consideration the value for the cement (55.64; Table S5), this value is interpreted to represent the change between the intertidal and subtidal conditions (Figs. 12A–E). There is a higher predominance of subtidal conditions that occur in sections to the south (Tizra 3 and 3-1), than in the northern sections (Fig. 12).

The vertical gradient I_1 can be compared directly and at the same scale as the stratigraphic sections (Fig. 3), and smaller frequency sequences (cycles) can be recognized within the S1 and S3 sequences. These sequences are deepening-shallowing cycles (possibly transgressive-regressive cycles), which are more marked in the northern sections, and with smaller fluctuations of the I_1 index than in the southern sections. The base of each cycle is defined in the shallowest values, although emersions do not occur. Six high-frequency cycles are recognized in sequence S1 (S1/1 to S1/6); sequence S2 remains unaltered with one cycle (S2/7); and sequence S3 has three cycles (S3/8 to S3/10). These cycles allow a more precise correlation of the sections, independent of their lithological nature (Fig. 3). Cycles range from 3.5 to 18.7 m thick, with an increased thickness to the south for S1/1, S1/3, S1/4, and S1/6, whereas the thickness increases to the north for S1/2, S1/5, S3/8, S3/9 (Table 3).

Taking into consideration that the early Brigantian substage, which constitutes a typical 3rd-order sequence/cycle of glacioeustatic origin, is about 330.34 to 332 Ma (using the absolute ages by Aretz et al., 2020), this would represent an interval of 1.66 Myr for the entire early Brigantian. For this duration, the sedimentation rate is 197.6 m per Ma, and the duration of the sequences S1 to S3 would be 610 ka. Since there are 10 cycles for this interval, each cycle would correspond to a period of 61 ka, a value which would be intermediate between the orbital obliquity and eccentricity cycles. However, if we use the geochronology published in Davydov et al. (2012), 330.9 to 332 Ma, the entire Brigantian would be 1.1 Myr, with a sedimentation rate of 298.2 m per Ma. In that case, each cycle would be 40.5 ka, which coincides closely with the orbital obliquity frequency. This coincidence, in contrast to the first approach of a tectonic control (mostly the numerous in the sequence S1 where faults are likely more active), suggest a more marked eustatic control on the platform, although owing to the similarity of facies in the pale grey microbial limestones, this parameter was virtually overlooked in the monotonous microbial facies.

9.3. Terrigenous inputs

It is recognised that a certain north-south turbidity gradient (Figs. 12F–J) exists, although in spite of the proximity to deltaic facies, the massive development of microbial mounds contrasts with the widely assumed hypothesis that this factor is one of the most important inhibitors for the growth of microbes in similar structures of the Mississippian (Lees and Miller, 1995; Leinfelder et al., 1996). Owing to the amount of grainstones and microbial limestones, the influence of this factor (above the basal beds and interbedded shales) in the sequences is not apparent for the limestones in the shelf. The occurrence of quartz grains is not all that important, even when forming the core of ooids, where bioclast fragments, peloids and small intraclasts are more common. Nevertheless, individual analysis for microbial and non-microbial facies suggests that turbidity (apart from energy) also is a dominant ecological control. The resulting values for I_2 are aligned in a narrow band, and no internal trends are recognized in the sections, even the values are more regrouped than for I_1, mostly for the deeper water sections. From the lower values (Table S5), there are palaeoberesellids, aoujgaliids and

calcifoliids which suggest that, at least, dysphotic conditions prevailed, whereas the occurrence of green algae (I_2 = 59.14) is selected as the constraint for the presence of euphotic conditions. Owing to the surrounding shales, the shallower-water samples are not necessary less turbid and more euphotic environments, which in some cases are located in deeper-water mound facies, free of clastic input landward (Cózar et al., 2019). This is the case for Tizra 3-1 and 3-2 (Figs. 12H–I), with many of the samples located in euphotic conditions, although the scarce samples of Tizra 3 gives a predominant dysphotic setting (Fig. 12J). Both settings seem to be of similar importance in the shallower-water sections (Tizra 3-3 and 3-4) (Figs. 12F–G). In general terms, dysphotic conditions predominate to the south and the euphotic conditions are predominant to the north, showing also a similar north-south gradient identified by field observations, facies analysis and index I_1.

Hence, according to the energy levels experienced by the shelf, it would coincide with the "middle and inner ramp" settings defined by Burchette and Wright (1992).

9.4. Controls on the development of ooids versus microbial boundstones

The occurrence of ooidal/bioclastic grainstones in the lower part of the succession, S1/1 to S1/3 in Tizra 3-3 section, seems to be controlled by the development of shoals landward over a smooth palaeorelief generated by tectonics, sea-level fall and decrease in terrigenous input, whereas the occurrence of rare and small microbial mounds can be only attributed to possible areas of lower energy in between, such as those described by Dilliar et al. (2010), or as sand bodies separated by wide deep channels extending to the platform edge (Fig. 11). Some of these grainstones spread seawards, and transported material from the shoals into deeper settings, mostly transported by storm episodes (e.g., Bathurst, 1975; Rankey et al., 2006), or more rarely gravity-driven flows seawards from the ooid shoals.

In cycles S1/4 to S1/6, a similar origin is inferred for most of the non-microbial beds. The shoal was located further to the north of Tizra 3-3 (Fig. 3), whereas in Tizra 3-3 to 3-1, mostly tempestites occur. It seems that the top of the microbial mounds reached, temporarily, intertidal conditions, allowing the incipient formation of the grainstone facies.

The cycle S2/7 contains deeper water conditions (Fig. 3), allowing a predominance of microbial mounds, and only very thin shoal deposits in the northeast outcrops (Tizra 3-4). This shoal deposits extend only into the top of the mound up to Tizra 3-3, whereas further to the south, only some storm events are recorded within the microbial facies, mostly at the base of the mounds. However, locally (Tizra 3-2), typical ooids are recorded as the base of nucleation for the mound. This more uniform facies distribution is a result of a more levelled platform, slightly deepening to the south, and the occurrence of ooidal grainstones or microbial mounds is interpreted to be mostly controlled by changes in sea level.

The cycle S3/8 is rather similar to S2/7, with a marked shallowing phase (Fig. 3), but in this case, the platform was more levelled and the shoal deposits were widely generated in each section. The cycle S3/9 is similar to S2/7, with a slight steepening to

the south, where the shallower part of the cycle is not represented in Tizra 3-1 and 3-2 sections, and thick typical shoals mostly present in Tizra 3-4. Cycle S3/10 is poorly represented, but it might be interpreted as S3/9.

Owing to the similar thicknesses and facies distribution, a glacioeustatic origin for the alternation of microbial mounds and oolites is more feasible for the upper part of the succession, whereas repetitive fault movements might be the main control during the deposition of sequence S1, with more marked thickness variations. However, the latter feature cannot be completely ruled out for the upper sequence S2, because slight variation in the steepness of the platform occurs, being only completely levelled for cycle S3/8, and slightly deeper to the south for the upper sequences. This glacioeustatic control on the distribution of facies would appear to be a similar mechanism to that presented by Tomás et al. (2013), Goldstein et al. (2013) or Suarez-González et al. (2019) for explaining similar alternation of oolitic and microbial lithologies. In particular, Goldstein et al. (2013) recognized a higher production of ooids related to pre-existing palaeotopography, which in the case of Tizra, this topography seems to be generated by the extensional faults, leaving the northern blocks more elevated, and thus, favouring the thicker accumulation of ooidal beds in sequences S2 and S3 in Tizra 3-3 and 3-4.

The occurrence of the ooidal grainstones-packstones is mostly localized in the shallowest part of the cycles, mainly those considered as recorded in situ, and rarely in the early stages of the deepening phase (Fig. 3), as recorded by Suarez-González et al. (2019). This predominance in the shallowing phases contrasts with Lehrman et al. (2020), who recorded most of their oolites in the transgressive deeper phases.

If the non-skeletal and skeletal components (including the ooid types) are compared with the facies/autochthony/shallowing-deepening cycles as variables, the resulting CCA gives us three main parameters controlling the occurrence of ooids (Fig. 13; Table S6). The first axis (IO_1, 42.76%) is related with the bathymetry, which is given in the order of typical shallower-water skeletal and non-skeletal components (including the six types of ooids) in the low values, as well as the highest levels with in situ generated ooids. In the opposite extreme, the levels with more transported ooids associated with deeper biota are recorded in the microbial facies.

The second axis (IO_2, 22.73%) is apparently a measure of the energy in the environment, and although in intermediate positions, but the variable deepening is close to the low values, and shallowing in highest values (together with the six types of ooids). Thus, it seems to confirm more energy in the environments during the shallowing phases. Nevertheless, the regular type 3 and irregular type 2 ooids are mostly concentrated in shallowing phases and precipitated in situ, whereas the compound ooids, and regular types 1 and 2 tend to be more easily transported and redistributed during the deepening phases (transgressive?) into the deeper microbial facies and tempestites. The third axis, of a certain relevance (15.53%), could not be identified. Thus, apart from oolitic grainstones developed in the top of mounds, the isolated ooids or those that accumulated in patches and veins seem to be all transported into the microbial facies, which contrasts with their generation within the microbial

communities of the buildups, due to higher levels of energy, as proposed by some previous authors (e.g., Ahr and Stanton, 1996; Villafañe et al., 2018).

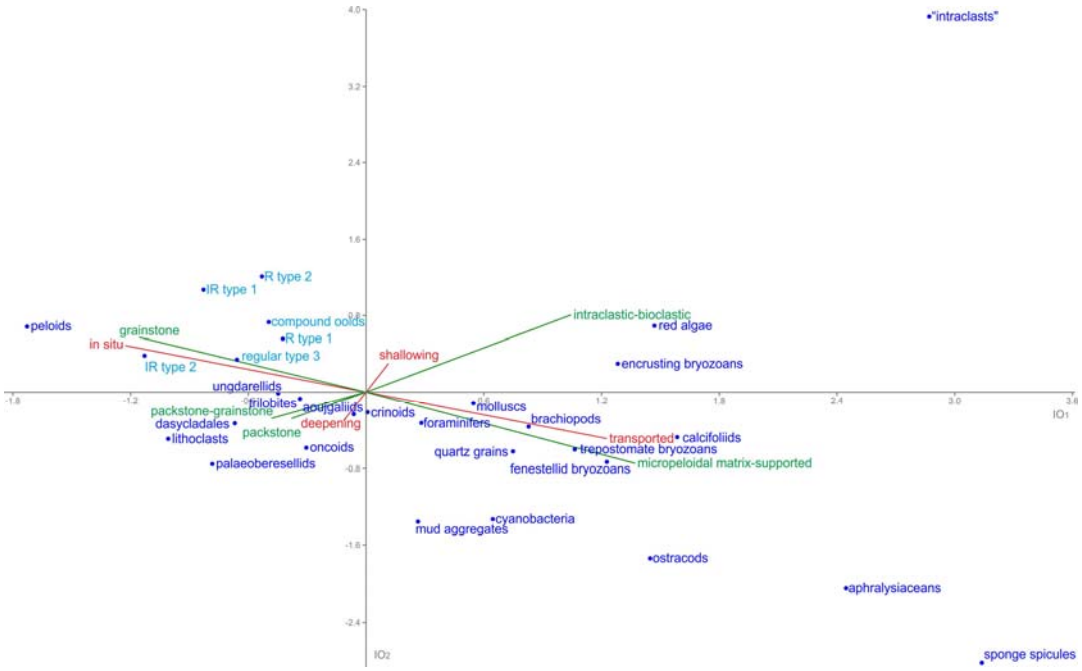

Fig. 13. Triplot CCA analysis (axes 1 and 2) for the samples with ooids using as variables the types of facies, TR cycles and the allochthony/autochthony.

11. Conclusions

The distribution in components during the alternation of microbial mounds and oolitic/bioclastic grainstone-packstone facies are primary controlled by the energy and turbidity of the environments, although turbidity is a more important factor for the microbial mounds. The levels assigned to higher energy in the mounds, correspond to the majority of tempestites in the platform. The latter also show a great influence on the distribution of nutrients, as well as a geochemical factor, which coincides with the higher production of ooids in the shallower-water facies. Those parameters suggest a gradient towards more open marine conditions from north to south (landwards to seawards), coinciding with the inferred bathymetric gradient for the platform.

The geometry and architecture of the platform, however, is conditioned by syn-sedimentary faults and the subsequent generation of accommodation space by tectonic subsidence, as well as the occurrence of stacked deepening-shallowing cycles coinciding in time with orbital obliquity cycles, and thus, a glacieustatic control seems to be also important.

The analysis of the ooids suggests that less than 40% of samples yield ooids generated in situ, whereas there is a predominance of transported ooids. Within the place of generation, it is confirmed that the large irregular and elongated ooids were generated in calmer water than the typical rounded and egg-shaped ooids. The occurrence of the predominant types of ooids in shallower-water grainstones with in situ

generation, and in the deepest-water microbial facies, suggest their facility to be transported. The higher production of ooids occurs during the shallowing phases of the cycles, whereas they were more easily transported during the deepening phases. No evidence of in situ generation of ooids within the microbial buildups is recognized, and all the specimens recorded in this setting are considered as transported.

Declaration of competing interest

The authors have no conflict of interest to declare and pledge that the submitted work is original.

Acknowledgments

We would like to thank M. Berkhli (Université de Meknès, Morocco) for field assistance in sampling. Financial support by the project CGL2016-78738 of the Spanish Ministry of Research and Innovation is acknowledged.

References

Adachi, N., Ezaki, Y., Liu, J., Cao, J., 2009. Early Ordovician reef construction in Anhui Province, South China: A geobiological transition from microbial- to metazoan-dominant reefs. Sedimentary Geology 220, 1–11.

Ahr, W.M., Stanton, R.J., 1996. Constituent composition of Early Mississippian carbonate buildups and their level-bottom equivalents, Sacramento Mountains, New Mexico. In: Strogen, P., Somerville, I.D., Jones, G.Ll. (Eds.), Recent Advances in Lower Carboniferous Geology. Geological Society Special Publication No. 107, pp. 83–95.

Allary, A., Lavenu, A., Ribeyrolles, M., 1976. Étude tectonique et microtectonique d'un segment de chaîne hercynienne dans la partie sud-orientale du Maroc central. Notes et Mémoires du Service géologique du Maroc 261, 1–169.

Allen, J.R.L., 1980. Sandwaves: a model of origin and internal structure. Sedimentary Geology 26, 281–326.

Aretz, M., Herbig, H.-G., 2008. Microbial-sponge and microbial-metazoan buildups in the late Viséan basin-fill sequence of the Jerada Massif (Carboniferous, NE Morocco). Geological Journal 43, 307–336.

Aretz, M., Herbig, H.G., Wang, X.D., 2020. The Carboniferous Period. In: Gradstein, F.M., Ogg, J.G., Schmitz, M.D., Ogg, G.M. (Eds.), Geologic Time Scale 2020. Elselvier. https://doi.org/10.1016/B978-0-12-824360-2.00023-1

Baccelle, L., Bosellini, A., 1965. Diagrammi per la stima visiva della composizione percentuale nelle rocce sedimentarie. Annali dell'Università di Ferrara, Sezione IX, Scienze Geologiche e Paleontologiche 1**,** 59–62.

Bathurst, R.G.C., 1975. Carbonate sediments and their diagenesis. Development in Sedimentology 12, 1–658.

Ben Abbou, M., Soula, J.C., Brusset, S., Roddaz, M., Ntarmouchant, A., Driouch, Y., Christophoul, F., Bouabdelli, M., Majesté-Menjoulas, C., Béziat, D., Debat, P., Deramond, J., 2001. Contrôle tectonique de la sédimentation dans le système de bassins d'avant-pays de la Meseta marocaine. Comptes Rendus Académie des Sciences, Paris 332, 703–709.

Berger, S., Kaever, M.J., 1992. Dasycladales: an illustrated monograph of a fascinating algal order. Georg Thieme, Stuttgart, 247 pp.

Berkhli, M., Vachard, D., Paicheler, J.C., 2001. Les séries du Carbonifère inférieur de la région d'Adarouch, NE du Maroc central: lithologie et biostratigraphie. Journal of African Earth Sciences 32, 557–571.

Bosence, D.W.J., 1983. Description and classification of rhodoliths (rhodoids, rhodolites). In: Peryt, T.M. (Ed.), Coated grains. Springer-Verlag, Berlin, pp. 217–224.

Bouabdelli, M., Piqué, A., 1996. Du bassin sur décrochement au bassin d'avant-pays: Dynamique du bassin d'Azrou-Khénifra (Maroc hercynien central). Journal of African Earth Sciences 23, 213–224.

Bourque, P.-A., Madi, A., Mamet, B.L., 1995. Waulsortian-type bioherm development and response to sea-level fluctuations: Upper Viséan of Béchar Basin, Western Algeria. Journal of Sedimentary Research 65, 80–95.

Braak, C.J.F. ter, Verdonschot, P.F.M., 1995. Canonical correspondence analysis and related multivariate methods in aquatic ecology. Aquatic Sciences 57, 255–289.

Burchette, T.P., Wright, V.P., 1992. Carbonate ramp depositional systems. Sedimentary Geology 79, 3–57.

Camoin, G., Cabioch, G., Eisenhauer, A., Braga, J.-C., Hamelin, B., Lericolais, G., 2006. Environmental significance of microbialites in reef environments during the last deglaciation. Sedimentary Geology 185, 277–295.

Carozzi, A.V., 1957. Contribution à l'étude des propriétés géométriques des oolithes – l'exemple du Grand Lac Salé, Utah, USA. Institut National Genève Bulletin 58, 1–52.

Carozzi, A.V., 1960. Microscopic Sedimentary Petrology. Wiley, New York, 485 pp.

Cózar, P., Somerville, I.D. 2016. Problems correlating the late Brigantian–Arnsbergian Western European substages within northern England. Geological Journal 51, 817–840.

Cózar, P., Rodríguez, S., Somerville, I.D., 2003. Large multi-biotic cyanoliths from relatively deep-water facies in the early Serpukhovian of SW Spain. Facies 49, 31–48.

Cózar, P., Somerville, I.D., Rodríguez, S., Mas, R. and Medina-Varea, P., 2006. Development of a late Viséan (Mississippian) mixed carbonate/siliciclastic platform in the Guadalmellato Valley (southwestern Spain). Sedimentary Geology 183, 269–295.

Cózar, P., Vachard, D., Somerville, I.D., Berkhli, M., Medina-Varea, P., Rodríguez, S., Said I., 2008. Late Viséan-Serpukhovian foraminiferans and calcareous algae from

the Adarouch region (central Morocco), North Africa. Geological Journal 43, 63–485.

Cózar, P., Said, I., Somerville, I.D., Vachard, D., Medina-Varea, P., Rodríguez, S., Berkhli, M., 2011. Potential foraminiferal markers for the Visean-Serpukhovian and Serpukhovian-Bashkirian boundaries – A case-study from Central Morocco. Journal of Paleontology 85, 1105–1127.

Cózar, P., Somerville, I.D., Coronado, I., Vachard, D., Izart, A., Aretz, M., 2018. States of preservation and role of dasycladal algae in Mississippian carbonate mounds. Palaios 33, 419–430.

Cózar, P., Izart, A., Somerville, I.D., Aretz, M., Coronado, I., Vachard, D., 2019. Environmental controls on the development of Mississippian microbial carbonate mounds and platform limestones in southern Montagne Noire (France). Sedimentology 66, 2392–2424.

Davies, P.J., Bubela, B., Ferguson, J., 1978. Formation of ooids, Sedimentology 25, 703–730.

Davydov, V.I., Korn, D., Schmitz, M.D. Gradstein, F.M., Hammer, O., 2012. Chapter 23 – The Carboniferous period. In: Gradstein, F.M., Ogg, J.G., Schmitz, M.D., Ogg, G.M. (Eds.), The Geologic Time Scale 2012. Elsevier, Amsterdam, pp. 603–651.

Devuyst, F.-X., Lees, A., 2001. The initiation of Waulsortian buildups in Western Ireland. Sedimentology 48, 1121–1148.

Diaz, M.R., Eberli, G.P., 2019. Decoding the mechanism of formation in marine ooids: A review. Earth-Sciences Reviews 190, 536–556.

Diaz, M.R., Swart, P.K., Eberli, G.P., Oehlert, A.M., Devlin, Q., Saeid, A., Altabete, M.A., 2015. Geochemical evidence of microbial activity within ooids. Sedimentology 65, 2090–2112.

Dilliar, K.A., Pope, M.C., Coniglio, M., Hasiotis, S.T., Lieberman, B.S., 2010. Active synsedimentary tectonism on a mixed carbonate-siliciclastic continental margin: third-order sequence stratigraphy of a ramp to basin transition, lower Sekwi Formation, Selwyn Basin, Northwest Territories, Canada. Sedimentology 57, 513–542.

Dunham, R.J., 1962. Classification of carbonate rocks according to depositional texture. In: Ham W.E. (Ed.), Classification of Carbonate Rocks. American Association of Petroleum Geologists, Memoir 1, 108–121.

Duguid, S.M.A., Kyser, T.K., James, N.P., Rankey, E.C., 2010. Microbes and ooids. Journal of Sedimentary Research 80, 236–251.

Dupraz, C., Reid, R.P., Braissant, O., Decho, A.W., Norman, R.S., Visscher, P.T., 2009. Processes of carbonate precipitation in modern microbial mats. Earth-Science Reviews 96, 141–162.

Flügel, E., 2004. Microfacies of carbonate rocks. Analysis, interpretation and application. Springer Verlag, Berlin, Heidelberg, NewYork, 984 pp.

Freeman, T., 1962. Quiet water oolites from Laguna Madre Texas. Journal of Sedimentary Petrology 32, 475–483.

Friedman, G.M., Amiel, A.J., Schneidermann, N., 1974. Submarine cementation in reefs: example from the Red Sea. Journal of Sedimentary Petrology 44, 816–825.

Ginsburg, R.N., Bosellini, A., 1973. Form and internal structure of recent algal nodules (rhodolites) from Bermuda: a reply. Journal of Geology 81, 239.

Goldstein, R.H., Franseen, E.K., Lipinski, C.J., 2013. Topographic and sea level controls on oolite-microbialite-coralgal reef sequences: The terminal carbonate complex of southeast Spain. American Association of Petroleum Geologists Bulletin 97, 1997–2034.

Graham, L.E., Wilcox L.W., 2000. Algae: Prentice Hall, Upper Saddle River, New Jersey, 640 pp.

Harris, P.M., Diaz, M.R., Eberli, G.P., 2019. The formation and distribution of modern ooids on Great Bahama Bank. Annual Review of Marine Science 11, 491–516.

Heller, P.L., Komar, P.D., Pevear, D.R., 1980. Transport processes in ooid genesis. Journal of Sedimentary Petrology 50, 943–952.

Hennebert, M., Lees, A., 1991. Environmental gradients in carbonate sediments and rocks detected by correspondence analysis: examples from the Recent of Norway and the Dinantian of southwest England. Sedimentology 38, 623–642.

Izart, A., Vachard, D., Berkhli, M., 2017. The Carboniferous Culm basins of Moroccan Meseta. LAP LAMBERT Academic Publishing, Saarbrücken, 51 pp.

Karim, A. 2008. Le système siliciclastique-carbonate de la marge Sud-Ouest paléotéthysienne au Viséen supérieur: enregistrements paléoenvironnementaux et évolution dans un bassin d'avant-pays (Tizra: Maroc Central). Thèse Université Paris Sud-XI, Orsay, 256 pp. (unpublished).

Lees, A., Miller, J., 1985. Facies variation in Waulsortian buildups, Part 2; Mid-Dinantian buildups from Europe and North America. Geological Journal 20, 159–180.

Lees, A., Miller, J., 1995. Waulsortian banks. In: Monty, C.L.V., Bosence, D.W.J., Bridges, P.H., Pratt, B.R. (Eds.), Carbonate mud-mounds: Their origin and evolution. International Association of Sedimentologists, Special Publication 23, 191–271.

Lees, A., Hallet, V., Hibo, D., 1985. Facies variation in Waulsortian buildups, Part 1; A model from Belgium. Geological Journal 20, 133–158.

Lehrmann, D.J., Droxler, A.W., Harris, P.M., Minzoni, M., Droxler, D.A., Hopson, H.H., Kelleher, C., Khanna, P., Lhermann, A.A., Lhemann, A., Mabry, G., Mercado, L., Proctor, J.M., Singh, P., Yazbek, L., 2020. Controls on microbial and oolitic carbonate sedimentation and stratigraphic cyclicity within a mixed carbonate-siliciclastic system: Upper Cambrian Wilberns Formation, Llano Uplift, Mason County, Texas, USA. The Depositional Record 6, 276-308.

Leinfelder, R.R., Werner, W., Nose, M., Schmid, D.U., Krautter, M., Laternser, R., Takacs M., Hartmann, D., 1996. Paleoecology, growth parameters and dynamics of coral, sponge and microbolite reefs from the Late Jurassic. In: Reitner, J., Neuweiler, F., Gunkel, F. (Eds), Global and regional controls on biogenic sedimentation. I. Reef evolution. Research Reports. Göttinger Arbeiten zur Geologie und Paläontologie 2, 227–248.

Miller, J., 1986. Facies relationship and diagenesis in Waulsortian mud mounds from the Lower Carboniferous of Ireland and N. England. In: Schroeder, J.H., Purser, B.H, (Eds.), Reef diagenesis. Springer Verlag, Berlin, pp. 311–335.

Palmer, M.W., 1993. Putting things in even better order: the advantages of canonical correspondence analysis. Ecology 74, 2215–2230.

Peryt, T.M., 1983. Classification of Coated Grains. In: Peryt, T.M. (Ed.), Coated Grains. Springer, Berlin, pp. 3–6.

Pickard, N.A.H., 1992. Depositional controls on Lower Carboniferous microbial buildups, eastern Midland Valley of Scotland. Sedimentology 39, 1081–1100.

Pille, L., 2008. Foraminifères et algues calcaires du Mississippien supérieur (Viséen supérieur-Serpukhovien): rôles biostratigraphique, paléoécologique et paléogéographique aux échelles locale, régionale et mondiale. Thèse Université de Lille 1, 3 volumes, 327 pp, 256 pp, 150 pp (unpublished).

Ramette, A., 2007. Multivariate analysis in microbial ecology. FEMS Microbiology Ecology 62, 142–160.

Rankey, E.C., Riegl, B., Steffen, K., 2006. Form, function and feedbacks in a tidally dominated ooid shoal, Bahamas. Sedimentology 53, 1191-1210.

Richter, K., 1983. Calcareous ooids: a synopsis. In: Peryt, T.M. (Ed.), Coated Grains. Springer, Berlin, pp. 71–99.

Rodríguez-Martínez, M., Reitner, J., Mas, R., 2010. Micro-framework reconstruction from peloidal-dominated mud mounds (Viséan, SW Spain). Facies 56, 139–156.

Shinn, E.A., Robbin, D.M., Lidz, B.H., Hudson, J.H., 1983. Influence on deposition and early diagenesis on porosity and chemical compactation in two Paleozoic buildups: Mississippian and Permian age rocks in the Sacramento Mountains, New Mexico. In: Harris, P.M., Carbonate Buildups - A core workshop. Society of Economic Palaeontology and Mineralogy Society for Sedimentary Geology 4, 182–222.

Somerville, I.D., Rodríguez, S., Said, I., Cózar, P., 2012. Mississippian coral assemblages from Tabainout mud-mound complex, Khenifra area, Central Morocco. Geologica Belgica 15, 308–316.

Steinhoff, I., Strohmenger, C., 1996. Zechstein 2 carbonate platform subfacies and grain-type distribution (Upper Permian, Northwest Germany). Facies 35, 105–132.

Suarez-González, P., Arenas, C., Benito, M.I., Pomar, L., 2019. Interplay between biotic and environmental conditions in pre-salt Messinian microbialites of the western Mediterranean (Upper Miocene, Mallorca, Spain). Palaeogeography, Palaeoclimatology, Palaeoecology 533, 109242.

Sun, S.Q., Wright, V.P., 1989. Peloidal fabrics in Upper Jurassic reefal limestones, Weald Basin, southern England. Sedimentary Geology 65, 165–181.

Tomás, S., Homann, M., Mutti, M., Amour, F., Christ, N., Immenhauser, A., Agar, S.M., Kabiri, L., 2013. Alternation of microbial mounds and ooid shoals (Middle Jurassic, Morocco): Response to palaeoenvironmental changes. Sedimentary Geology 294, 68–82.

Trower, E.J., Lamb, M.P., Fischer, W.W., 2017. Experimental evidence that ooid size reflects a dynamic equilibrium between rapid precipitation and abrasion rates. Earth and Planetary Science Letters 468, 112–18.

Vachard, D., Cózar, P., 2010. An attempt of classification of the Palaeozoic incertae sedis Algospongia. Revista Española de Micropaleontología 42, 129–241.
Vachard, D., Cózar, P., Aretz, M., Izart, A. 2016. Late Viséan-early Serpukhovian cyanobacteria and algae from the Montagne Noire (France); taxonomy and biostratigraphy. Bulletin of Geosciences 91, 433–466
Villafañe, P.G., Corbí, H., Cónsole-Gonella C., Ruiz-Sánchez, F.J., Soria, J.M., 2018. The Messinian stromatolites of the Sierra del Colmenar (Western Mediterranean): facies characterization and sedimentological interpretation. PeerJ 6, e5766.
Whalen, M.T., Day, J., Eberli, G.P., Homewood, P.W., 2012. Microbial carbonates as indicators of environmental change and biotic crises in carbonate systems: examples from the late Devonian, Alberta basin, Canada. Palaeogeography, Palaeoclimatology, Palaeoecology 1981, 127–151.
Wendt, J., Kaufmann, B., Belka, Z., 2001. An exhumed Palaeozoic underwater scenery: the Visean mud mounds of the eastern Anti-Atlas (Morocco). Sedimentary Geology 145, 215–233.
Wray, J.L., 1977. Late Paleozoic calcareous red algae: In: Flügel, E. (Ed.), Fossil Algae. Recent Results and Developments. Berlin, Springer-Verlag, pp. 167–176.
Wright, V.P., 1992. A revised classification of limestones. Sedimentary Geology 76, 177–185.

Supplementary Material_ Methodology

Alternating microbial mounds and ooidal shoals as a response to tectonic, eustatic and ecological conditions (late Viséan, Morocco): Methodology

Pedro Cózar[a,b,*], Ismael Coronado[c], Alejandra García-Frank[b], Alain Izart[d], Ian D. Somerville[e], Daniel Vachard[f]

[a] *Instituto de Geociencias CSIC-UCM, c/ Severo Ochoa 7, 28040, Madrid, Spain*
[b] *GEODESPAL, Universidad Complutense de Madrid, c/ José Antonio Novais, 12, 28040-Madrid, Spain*
[c] *Facultad de Ciencias Biológicas y Ambientales, Universidad de León, Campus de Vegazana s/n, 24071-León, Spain*
[d] *202 chemin de Cabanis, 34730 Prades-le-Lez, France*
[e] *UCD School of Earth Sciences, University College Dublin, Ireland*
[f] *1 rue des Tilleuls, 59152 Gruson, France*

* Corresponding author
E-mail: p.cozar@igeo.ucm-csic.es

The lower carbonate-rich part of the TZ2 Member (Fig. 2) is recognized from south to north along strike, but it occurs discontinuously with limestones ranging in thickness, from 20 m to 140 m thick, and overlain by approximately 100 m of shales in the upper part of the member. The carbonates are more common in the northern outcrops, whereas, in the southern outcrops, where the succession has been studied, there are more than 2 km without carbonates, and the member is exclusively formed by 200 m of shales. Only in the southern region are oolitic limestones (10 m thick) recorded in the middle-upper part of the TZ2 Member (Cózar et al., 2008), about 40 m below the top of the shales (boundary between the TZ2 and TZ3 members; Tizra 4 and 4-2 sections in Figs. 2–3).

In order to analyse the Tizra Formation, fourteen sections have been measured and sampled in the southern outcrops of the Tizra hills (Fig. 3), of which, Tizra 2, 3, 4 and 5 were previously studied (Cózar et al., 2008). This study is focused on the lower half of the TZ2 Member which is represented specifically by the Tizra 3, 3-1, 3-2, 3-3 and 3-4 sections (Figs. 3–4). Currently, the progress in the work of the quarry at Tizra 3 section (originally measured in 2002), has destroyed the outcrop, being back-filled by rubbish and limestone blocks, and thus, it could not be re-sampled in detail. In the upper half of the member, four sections were also measured, but they contain only ooidal bars (Tizra 4 and 4-2), small satellite microbial mounds and breccias (Figs. 2–3). The sections in the TZ3 Member have allowed the characterization of typical microbial mounds without alternation with ooids and bioclastic beds, and thus, they are excluded from this study.

The sampling interval in Tizra 3 sections is more or less uniform, approximately every 2 m, but when marked facies changes were observed in the field, to coincide with the base or top of mounds with marked stratification surfaces, the interval between samples was slightly reduced (Fig. 4). In those more uniform, apparently homogeneous, pale grey, fine-grained limestones, the 2 m-thick interval was respected, in order to maintain a random grid sampling and a random representation of the facies. In total c. 180 large thin-sections (50 x 80 mm) have been prepared. The carbonate microfacies were determined under the petrological microscope, using the classification of Dunham (1962) in recognising the components and textures for the non-microbial limestones, whereas the terms employed by Sun and Wright (1989), Wright (1992), and Rodríguez-Martínez et al. (2010) were used in describing the microbial limestone facies. The abundance of grains, cement and matrix was visually estimated using the charts of Baccelle and Bosellini (1965). Skeletal and non-skeletal components are used (Supplementary material – Table S1) as defined by Flügel (2004), except for the problematic Algospongia, in cases considered as red algae or green algae (Vachard and Cózar, 2010), as well as the particular features of the beds yielding in situ generation of ooid (Supplementary material – Table S2). Although many fossils are grouped into major biotic elements, the details of some of them were previously distinguished at genus and/or species levels, such as the aoujgaliids, dasycladales, aphralysiaceans, calcifoliids, red algae, cyanobacteria and foraminifers, which were described in Cózar et al. (2008, 2011). Palaeoberesellids (*Palaeoberesella*, *Exvotarisella* and *Kamaena*) also include the donezellids (*Kamaenella* and *Praedonezella*) to get a wider representation (Supplementary material – Table S1), due to their similarity in ecological associations (Cózar et al., 2019).

Canonical correspondence analysis methodology

For the analysis of the predominant ecological factors in the succession, the database obtained by mean of petrographic quantification has been reinterpreted by a Canonical correspondence analysis (CCA), using the methodology explained in detail in Cózar et al. (2019; and references therein). Just as was employed in Cózar et al. (2019), coarse-grained rudstone horizons are removed (comprising only two intraformational breccias) from the analysis, because the predominance of lithoclasts produces strong noise, conditioning the position of this non-skeletal component in the graphics. The main difference in the methodology compared to the previous study is that here, all those variables that were not present in at least 10% of the samples have been filtered out (versus 5%). This filtering is a method of reduction of noise in the database, and because it has been widely demonstrated that those few represented variables do not have a great influence on the results (ter Braak and Verdonschot, 1995). Another difference is that the micropeloids have not been quantified independently, and they have been grouped under the term automicrites (sensu Reitner, 1993; Reitner and Neuweiller, 1995; Lees and Miller, 1995; Webb, 1999). In addition, the category of the lithoclasts has been separated in two groups: (i) lithoclasts sensu stricto, derived from

shallow water limestones (commonly in grainstones and packstones), and (ii) "intraclasts", as small and irregular micritic lithoclasts recorded in the microbial facies, and with an origin which seems to indicate automicrites cemented in the mounds. The CCA analysis was undertaken in two steps.

The first CCA analysis was performed exclusively for the non-microbial facies (NMCCA; Table S3) and the microbial facies (MCCA; Table S4), with the aim of avoiding plausible influence of interrelated factors, such as energy, which clearly controlled the distribution of grainstones and packstones. The CCA gives us some axes, which have been recalculated by means of the projections of the scores on the axes, and ordered from 0 to 100 in the samples and variables. These allow us to obtain ecological gradients, of which, only some axes are considered relevant for the explanation of the distribution. The values of the gradients for each sample can be plotted with the position of the samples, and thus, giving in pertinent cases, a vertical variation of the gradients. To analyse all the samples as a whole, might mask the influence of energy just within the microbial facies or, in contrast, assuming that all the grainstone and packstone facies are of a high energy, to mask the real ecological factors controlling their distribution. In this case, only samples with more than 40% of microbial textures and fabrics have been considered for the MCCA, and samples with less than 40% for the NMCCA. The reduced variables in the MCCA (< 10%) are: peloids, compound ooids, muddy aggregates, lithoclasts, bryopsidales, sponges, trilobites, solenoporaceans, rugose corals, tabulate corals, heterocorals and calcispheres. Four axes and their recalculated indices (IM_1, IM_2, IM_3, and IM_4) explain more than 90% of the variations. For the NMCCA, apart from all those absent components, other reduced variables (<10%) are mudstone-wackestone textures, intraclasts, peloids, red algae, sponge spicules, solenoporaceans and tabulate corals. In this case, due to their abundances, the palaeoberesellids are considered apart from the donezellids.

A single main axis results (INM_1) for all the non-microbial samples, which itself explain 85.93% of the variation, similarly as for the samples with in situ generation of ooids (ISO_1), which explain 100% of the variation. In both indices, the component and textures are ordered as a function of the percentage in allomicrite, and thus, both are interpreted as depending on the input of muddy material in suspension (turbidity). Based on the allomicrite distribution, vertical variation of INM_1 (Fig. 9) give a clear separation of the samples coinciding with levels attributed to tempestites from the oolitic shoals, using a level of separation value 40, where the packstone-grainstone facies occurs (Table S3) and as first texture yielding matrix.

For the microbial facies, the IM_1 index show a similar ordination of the components, textures and fabrics, depending on the percentage of allomicrite, and similarly is interpreted as the turbidity in the environment. The vertical gradient of this index (Fig. 10A–D), shows a marked change above the position of the dasycladales (at 22.8; Table S4), which are considered the most turbid environments. The IM_2 index is interpreted as a measure of the energy in the microbial mounds, where typical low-energy components (e.g., *Terebella*-like tubes, sponge spicules, agglutinated foraminifers and thin-walled ostracods) are ordered in the low values, whereas, in the higher values are observed "intraclasts", ungdarellids, aoujgaliids, ooids or brachiopods.

The vertical gradient suggests two values in the ordination, the occurrence of micrite (at 29.27; Table S4) and the cement (at 42.14), which allow to distinguish two boundary approximately at 30 and 40 (Fig. 10E–H), delimiting samples from low-moderate-high energy. The IM_3 index show most of the macrofossils depending on the nutrients inputs in the platform in the high values, whereas other components, independent of nutrients as well as most of algae (which are only photic dependent) are situated in the low values. The vertical gradient can be divided by the occurrence of allomicrite at 42.8 and micrite at 50.07, which can be split in zones at 42 and 50, where the component completely independent on nutrients are situated below 42, and those more depending on nutrients are above 50, with an intermediate zone (Fig. 10I–L). The IM_4 index show the organisms with stronger calcification of the wall in the low values, whereas that to higher values, there are recorded organism of agglutinated or siliceous walls, as well as those supposedly formed by high-magnesium or aragonitic walls, and thus, it is assumed that the index is a quantification of a chemical element favouring strong calcification, most probably the magnesium. Obviously, depending on the database, there are components in anomalous positions within the axes, but they are considered as statistical artifacts, and only the general trends are considered for the interpretation of the indices.

In the second step, a CCA analysis was performed for all the samples (Table S5); CCA gives us some axes, which have been recalculated by means of the projections of the scores on the axes, and ordered from 0 to 100 in the samples and variables. Only two axes are considered relevant for the explanation of the succession, axis 1 (represented by the index I_1), and axis 2 (represented by I_2), explaining that both together account for more than 80% of the variations. The filtered out components in the CCA are peloids, muddy aggregates, compound ooids, bryopsidales, sponges, solenoporaceans, rugose corals, tabulate corals, heterocorals, trilobites and calcispheres. The index I_1 is interpreted as a measure of the bathymetry/energy, whereas index I_2 is interpreted as the turbidity in the environment, showing similar component/textures distribution than in indices IM_2 and IM_1 respectively. Facing the individual data from each sample with its position in the stratigraphic sections, these indices allow us to obtain vertical ecological gradients (Fig. 12), where the shallow water facies are located at the value of the cement at 54.64. Owing to the overall facies in the platform, this boundary seems to separate the intertidal allowing cement precipitation from the subtidal facies with more common micrite accumulation and microbial production. On the other hand, in the turbidity gradient, the dasycladales marks again the euphotic levels at 59.14, separating the less turbid environments in the higher values (Fig. 12), whereas the other samples are interpreted as representative of dysphotic conditions. Completely aphotic environments do not occurs, because even between the lower values of the index, there are problematic algae, such as aoujgaliids or palaeoberesellid, photic-dependent, and frequently misinterpreted as red algae and dasycladales respectively.

In addition, a final CCA analysis has been done for samples yielding ooids (Supplementary material – Table S6), where different types of ooids have been quantified, as well as different features of the ooids. Three main indices have been obtained and recalculated (IO_1, IO_2 and IO_3), although some selected CCA analyses

have been performed on this database to compare different features. For this database, some changes introduced are the regrouping of the micropeloidal intraclastic-bioclastic and cement-supported subfacies and on the other hand, the micropeloidal matrix-supported and micritic subfacies. Index IO_1 is interpreted as the bathymetry where typical shallow water components are recorded, such as the peloids, dasycladales (mostly *Koninckopora* and *Nanopora*), and palaeoberesellids (mostly *Kamaenella*) within the grainstone facies. In this case, the bathymetry can be distinguish from the energy, represented by index IO_2, which although it shows a similar ordination of variables (but inverted compared to IO_1; Table 6), but it is observed a predominance of the larger and more energetic ooids in the higher values, as well as the components typically associated to higher energy, such as red algae, encrusting bryozoans and ungdarellids (also frequently interpreted as red algae). In contrast, IO_3 could not be identified.

References

Baccelle, L., Bosellini, A., 1965. Diagrammi per la stima visiva della composizione percentuale nelle rocce sedimentarie. Annali dell'Università di Ferrara, Sezione IX, Scienze Geologiche e Paleontologiche **1,** 59–62.

Braak, C.J.F. ter, Verdonschot, P.F.M., 1995. Canonical correspondence analysis and related multivariate methods in aquatic ecology. Aquatic Sciences 57, 255–289.

Cózar, P., Vachard, D., Somerville, I.D., Berkhli, M., Medina-Varea, P., Rodríguez, S., Said I., 2008. Late Viséan-Serpukhovian foraminiferans and calcareous algae from the Adarouch region (central Morocco), North Africa. Geological Journal 43, 63–485.

Cózar, P., Said, I., Somerville, I.D., Vachard, D., Medina-Varea, P., Rodríguez, S., Berkhli, M., 2011. Potential foraminiferal markers for the Visean-Serpukhovian and Serpukhovian-Bashkirian boundaries – A case-study from Central Morocco. Journal of Paleontology 85, 1105–1127.

Cózar, P., Izart, A., Somerville, I.D., Aretz, M., Coronado, I., Vachard, D., 2019. Environmental controls on the development of Mississippian microbial carbonate mounds and platform limestones in southern Montagne Noire (France). Sedimentology 66, 2392–2424.

Dunham, R.J., 1962. Classification of carbonate rocks according to depositional texture. In: Ham W.E. (Ed.), Classification of Carbonate Rocks. American Association of Petroleum Geologists, Memoir 1, 108–121.

Flügel, E., 2004. Microfacies of carbonate rocks. Analysis, interpretation and application. Springer Verlag, Berlin, Heildelberg, NewYork, 984 pp.

Lees, A., Miller, J., 1995. Waulsortian banks. In: Monty, C.L.V., Bosence, D.W.J., Bridges, P.H., Pratt, B.R. (Eds.), Carbonate mud-mounds: Their origin and evolution. International Association of Sedimentologists, Special Publication 23, 191–271.

Reitner, J., 1993. Modern cryptic microbialite/metazoan facies from Lizard Island (Great Barrier Reef, Australia) formation and concepts. Facies 29, 3–39.

Reitner, J., Neuweiler, F., 1995. Mud mounds: a polygenetic spectrum of fine-grained carbonate buildups. Facies 32, 1–70.
Rodríguez-Martínez, M., Reitner, J., Mas, R., 2010. Micro-framework reconstruction from peloidal-dominated mud mounds (Viséan, SW Spain). Facies 56, 139–156.
Sun, S.Q., Wright, V.P., 1989. Peloidal fabrics in Upper Jurassic reefal limestones, Weald Basin, southern England. Sedimentary Geology 65, 165–181.
Vachard, D., Cózar, P., 2010. An attempt of classification of the Palaeozoic incertae sedis Algospongia. Revista Española de Micropaleontología 42, 129–241.
Webb, G.E., 1999. Youngest Early Carboniferous (late Visean) shallow-water patch reefs in Eastern Australia (Rockhampton Group, Queensland): combining quantitative micro- and macro-scale data. Facies 41, 111–140.
Wright, V.P., 1992. A revised classification of limestones. Sedimentary Geology 76, 177–185.